

Late Neoproterozoic Granitoid Magmatism of the Baikal-Muya Fold Belt, Ophiolite and Post-Ophiolite Plagiogranites

A. V. Somsikova^{a, b, *}, Yu. A. Kostitsyn^a, A. A. Fedotova^b, A. A. Razumovskiy^b, E. V. Khain^b,
O. V. Astrakhantsev^a, V. G. Batanova^{a, c}, and M. O. Anosova^a

^a*Vernadsky Institute of Geochemistry and Analytical Chemistry, Russian Academy of Sciences,
ul. Kosygina 19, Moscow, 119991 Russia*

^b*Geological Institute (GIN), Russian Academy of Sciences, Pyzhevskii per. 7, Moscow, 109017 Russia*

^c*Université Grenoble Alpes, Institute Science de la Terre (ISTerre), CNRS, F-38041 Grenoble, France*

*e-mail: alinaorlova87@gmail.com

Received February 28, 2019; revised July 10, 2020; accepted July 10, 2020

Abstract—Three different-age series of granitoid veins and dikes of the Baikal–Muya fold belt were studied. Two of them, plagiogranites of the ophiolite complex and the first postophiolitic plagiogranites, are associated with the suprasubduction ophiolites of the eastern Baikal–Muya belt. The third series is represented by hypabyssal tonalite–plagiogranite–leucogranite complex of the Kichera zone in the western Baikal–Muya belt. The composition and isotope-geochemical characteristics ($\epsilon_{\text{Nd}}(\text{T}) = -0.9; -1.3$) of the plagiogranite veins no more than 60 cm thick, and $\epsilon_{\text{Nd}}(\text{T})$ values ($-1.8...+0.2$) of host layered leucocratic gabbros in the Sredne–Mamakan ophiolitic complex are consistent with the previously established suprasubduction nature of the ophiolite association. Tonalites and plagiogranites of the dyke system of the post-ophiolitic magmatic series intersect the dunite–pyroxenite–gabbro banded series of the Sredne–Mamakan ophiolites of the eastern Baikal–Muya fold zone. High Sr/Y ratios and low concentrations of Y and heavy REE indicate that these granitoids are ascribed to the adakite series. LA-ICP-MS study of zircon from post-ophiolitic plagiogranites yields the crystallization age of 629 ± 5 Ma. Sm–Nd isotope-geochemical characteristics of plagiogranitoids ($\epsilon_{\text{Nd}}(\text{T}) = +2.5; +4.0$) in combination with geochemical data confirm their origin during partial melting of a mafic protolith corresponding to the Neoproterozoic oceanic crust. The adakitic granitoids in the Kichera zone of the western Baikal–Muya belt belong to the tonalite–leucogranite differentiated series of the hypabyssal complex, which has no a direct spatial relationship with unambiguous ophiolite associations. The chemical composition and Sm–Nd isotope-geochemical characteristics of these rocks ($\epsilon_{\text{Nd}}(\text{T}) = +3.2...+7.1$) indicate the heterogeneity of the predominantly juvenile island-arc or oceanic Neoproterozoic crust, which experienced partial melting at 595 ± 5 Ma.

Keywords: plagiogranites, adakites, ophiolites, geochronology, zircon, Neoproterozoic, Baikal–Muya fold belt, Central Asian fold belt

DOI: 10.1134/S0016702921010109

INTRODUCTION

Many ophiolite complexes comprise plagiogranites, which are traditionally regarded as end product of differentiation of mafic magmas (Coleman, 1979; Savelieva et al., 2008). Granitoid derivatives frequently intrude gabbroids or sometimes form small intrusive stocks or separate dikes within dolerite sheeted dike complex (Khain et al., 2008; Ryazantsev et al., 2015; Furnes and Dilek, 2017). Using modern spreading ridges and ophiolite complexes as examples, it was proposed that acid magmas are formed by partial melting of hydrothermally altered basalts and gabbroids (Silantsev et al., 2014; Furnes and Dilek, 2017).

At the same time, it was established that some leucocratic intrusions postdate ophiolite complexes. These rocks could have adakitic affinity, i.e., are high-

Al sodic rocks with high Sr and low Y and HREE contents. Their origin is thought to be related to the partial melting of mafic protolith in equilibrium with garnet (Drummond et al., 1996; Turkina, 2002; Luchitskaya, 2002; Condie, 2005; Martin et al., 2005; Efremov, 2010). Adakites are formed within a narrow range of conditions and therefore are important geodynamic marker, which indicates an age of partial melting of the mafic oceanic lithosphere in deep subduction zones (Defant and Drummond, 1990; Defant and Kepezhinskas, 2001, and others) or lower crustal melting of thick continental crust above subduction zone (Petford, Atherton, 1996), or beyond an active subduction system (Xu et al., 2002, and others).

The determination of relations of plagiogranites with rocks of ophiolite complex, their indicator geo-

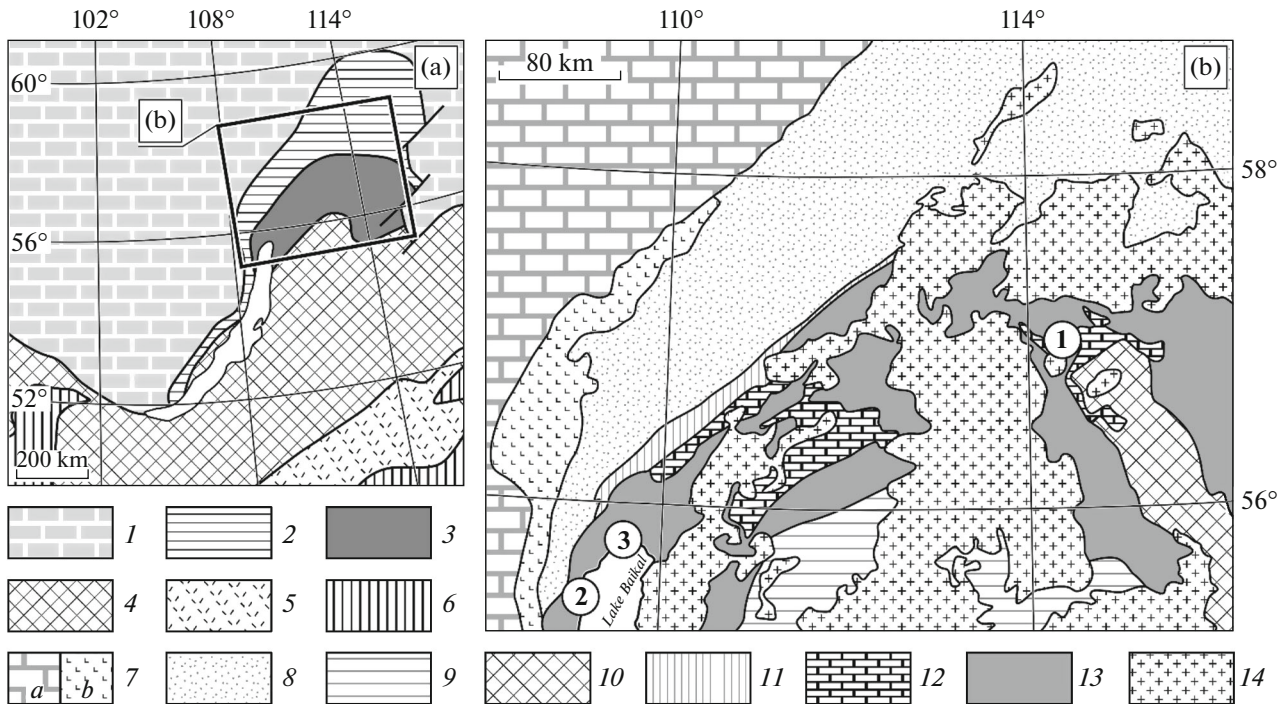


Fig. 1. Position of the studied objects in the geological structure of the region. (a) Tectonic scheme of the southern framing of the Siberian Platform. Compiled after (Parfenov et al., 2003, 2010). (b) Geological scheme of the Northern Baikal region and Transbaikalia. Modified after (Konnikov et al., 1999; Fedotova et al., 2014). (1) Siberian platform; (2) Baikal–Patom Belt; (3) Baikal–Muya Belt; (4) Yenisei–Transbaikalian Belt; (5) Mongol–Okhotsk Belt; (6) Tuva–Mongolian and Argun superterrane; (7) Siberian Platform: (a) cover, (b) basement consisting of the Akitkan volcanoplutonic belt; (8) Baikal–Patom Belt; (9) Kotera Zone consisting of the volcanosedimentary complexes of the Kotera and Gorblyok formations; (10–13) Baikal–Muya Belt: (10) Muya Block; (11) Synnyr rift structure, (12) Vendian–Lower Cambrian carbonate complexes, (13) undivided magmatic and metamorphic complexes of the Baikal–Muya Belt; (14) Paleozoic granitoids. Circled numerals show the studied areas: (1) Sredne-Mamakan massif, (2) Slyudyanka–Rel interfluvium; (3) coastal part of the northern termination of Lake Baikal, between the Cape of Kurla (NE margin of Severobaikal'sk) and left bank of the Turkin River.

chemical and isotope parameters, age, source composition and genesis of plagiogranites, provides insight into the geological evolution of convergent plate margins.

These problems are solved by the example of the Sredne-Mamakan ophiolite complex (Konnikov and Tsygankov, 1992; Konnikov et al., 1994; Perelyaev, 2003; Tsygankov, 2005) located in the Karalon–Mamakan zone of the eastern Baikal–Muya fold belt (Figs. 1, 2). A typical ophiolite rock association is recovered in tectonic sheets and nappes in the western part of the Middle Vitim highland within the Mamakan Block of the Karalon–Mamakan zone. “All they are restricted to the Yakor’–Kaaluu suture zone, which is the analogue and western continuation of the Yangudo–Param strike-slip–thrust “suture” “(Perelyaev, 2003, p. 7). The base of the section is made up of ultramafic rocks and serpentinites of the Kaalu “massif”, which is restricted to the Kaalu–Sredniy Mamakan watershed. Peridotites and gabbros of the layered complex are recovered within the Sredne-Mamakan “massif” occupying an area over 100 km² in the Sredniy–Pravyy Mamakan interfluvium (Fig. 2). Following age estimates were obtained for the

Sredne-Mamakan “massif” of the eponymous ophiolite complex:

(1) mineral isochron age (*OPx*, *CPx*, *Pl*) of 704 ± 71 Ma for leucocratic gabbro-norites (Rytsk et al., 2001),

(2) isochron age of 774 ± 67 Ma on four rock samples from a rhythm of layered series (clinopyroxenites, gabbroids, including leucocratic gabbro-norites with minerals of the above isochron determination) (Rytsk et al., 2001);

(3) SHRIMP zircon ages of 640 ± 4 and 650 ± 6 Ma for two considered below plagiogranite dikes of the Mamakan ophiolite association (Kröner et al., 2015).

The rocks of the Sredne-Mamakan “massif” are ascribed to the 0.7–0.8-Ga stage of the formation of layered plutons (Rytsk et al., 2007). At the same time, the Sredne-Mamakan ophiolite association, which includes the eponymous and Kaalu massifs (further, massifs are referred to as traditionally distinguished units of fold belt with intrusive or tectonic contacts) is interpreted as relict crust of marginal sea (Stanevich and Perelyaev, 1997; Perelyaev, 2003) or as island-arc ultramafic–mafic massif (Tsygankov, 2005).

The study object is plagiogranites, which have cross-cutting relations with rocks of the dunite–

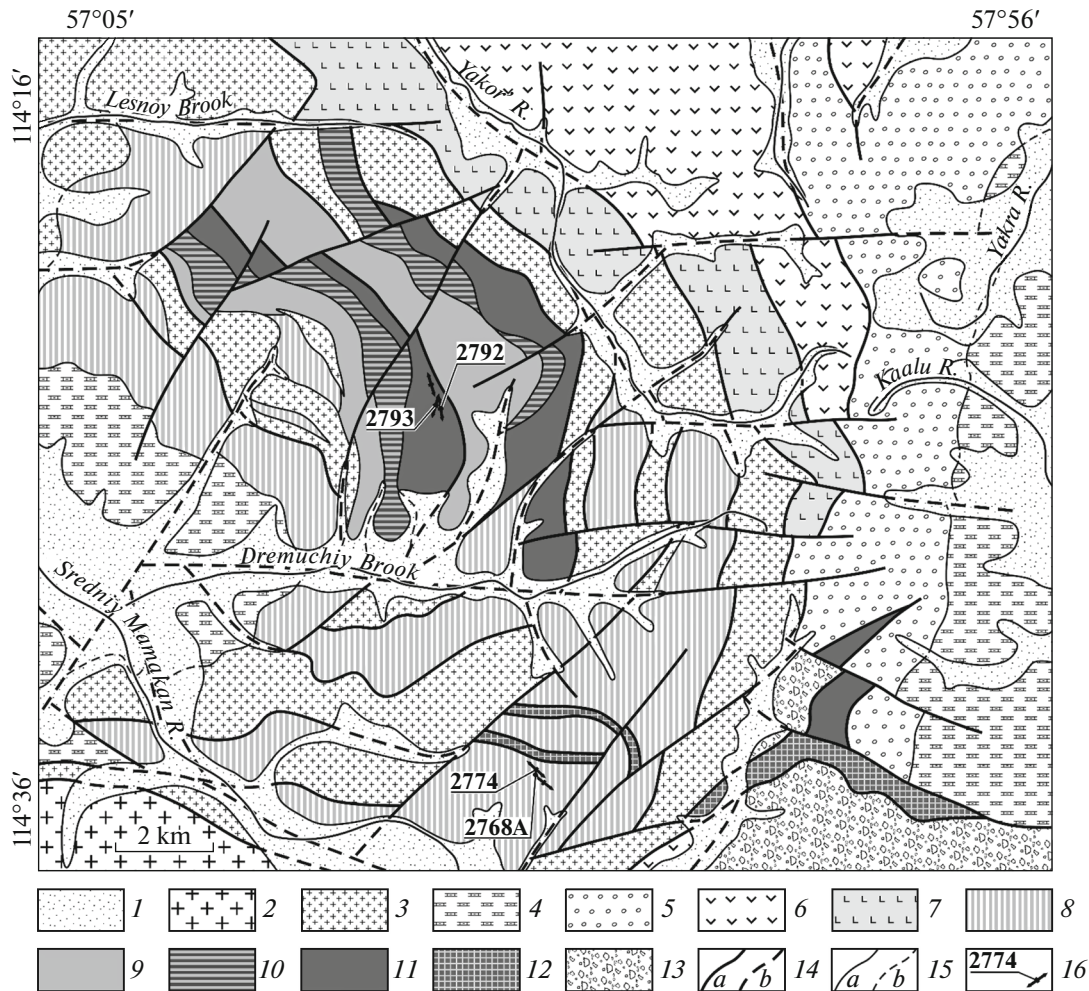


Fig. 2. Geological scheme of the Sredne-Mamakan ophiolite massif. Compiled after (Perelyaev, 2003; Stanevich and Perelyaev, 1997). (1) Quaternary alluvial–proluvial sediments; (2) Paleozoic granitoids; (3) Vendian granites, granodiorites, and diorites of the Lesnoy Complex; (4) Vendian–Cambrian carbonate–clastic rocks; (5) Riphean–Vendian coarse–clastic graywackes; (6) Riphean–Vendian Yakor volcanosedimentary group; (7–12) Sredne-Mamakan ophiolite association: (7) gabbrodolerite, dolerite (veins and dikes), basalts, cherts, (8) amphibole gabbro, (10) olivine gabbro and partially silicitized gabbro, (9) gabbronorite and gabbro, (10) olivine melanogabbro, gabbronorite, and gabbro, (11) wehrlite, dunite, olivine melanogabbro, troctolite, (12) dunite–harzburgite complex, (13) tectonic (terrigenous, polymictic) mélangé; (14) faults: (a) proved, (b) inferred; (15) geological boundaries: (a) proved, (b) inferred; (16) granitoid veins (off-scale), localities and sample numbers; plagiogranites sample 2768A (56°57.172' N, 114°26.74' E), sample 2774 in the Sredne-Mamakan ophiolite association (coordinates given earlier in the article Kröner et al., 2015); tonalities sample 2792 (57°01.020' N, 114°23.885' E), plagiogranites sample 2793 from dikes in the upper reaches of the Dremuchiy Brook, which cut across dunite–pyroxenite–gabbro of the banded complex of the Sredne-Mamakan ophiolite association (57°01.056' N, 114°23.875' E; coordinates are given in the Pulkovo 1942 system).

pyroxenite–gabbro banded series of the Sredne-Mamakan ophiolite complex. They are compared with plagiogranites of the Sredne-Mamakan ophiolite association, and granitoid dikes of the Kichera zone in the western Baikal–Muya belt, which geochemically correspond to adakites (Figs. 1, 3).

NEOPROTEROZOIC GRANITOID DIKES IN THE BAIKAL–MUYA BELT

Several distribution zones of Neoproterozoic island-arc metavolcanic rocks and ophiolite complexes (Fig. 1) in association with gabbroids, granitoids, and sedimentary rocks of different age are distin-

guished in the Baikal–Muya fold belt (Klitin et al., 1975; Dobretsov, 1983; Tsygankov, 1998). These zones border with complexes of a Neoproterozoic paleobasin formed on the Siberian margin (Fig. 1).

The metavolcanics and ophiolite association rocks are most abundant in the Mamakan and Tallain blocks of the Karalon–Mamakan zone in the east (Dobretsov et al., 1992; Konnikov et al., 1994; Rytsk et al., 2001) and in the Kichera zone in the west of the Baikal–Muya fold belt (Konnikov et al., 1999, Tsygankov, 2005, and others). The metavolcanics in the Karalon–Mamakan zone are represented by volcanosedimentary rocks of the Karalon and Yakor' sequences, while

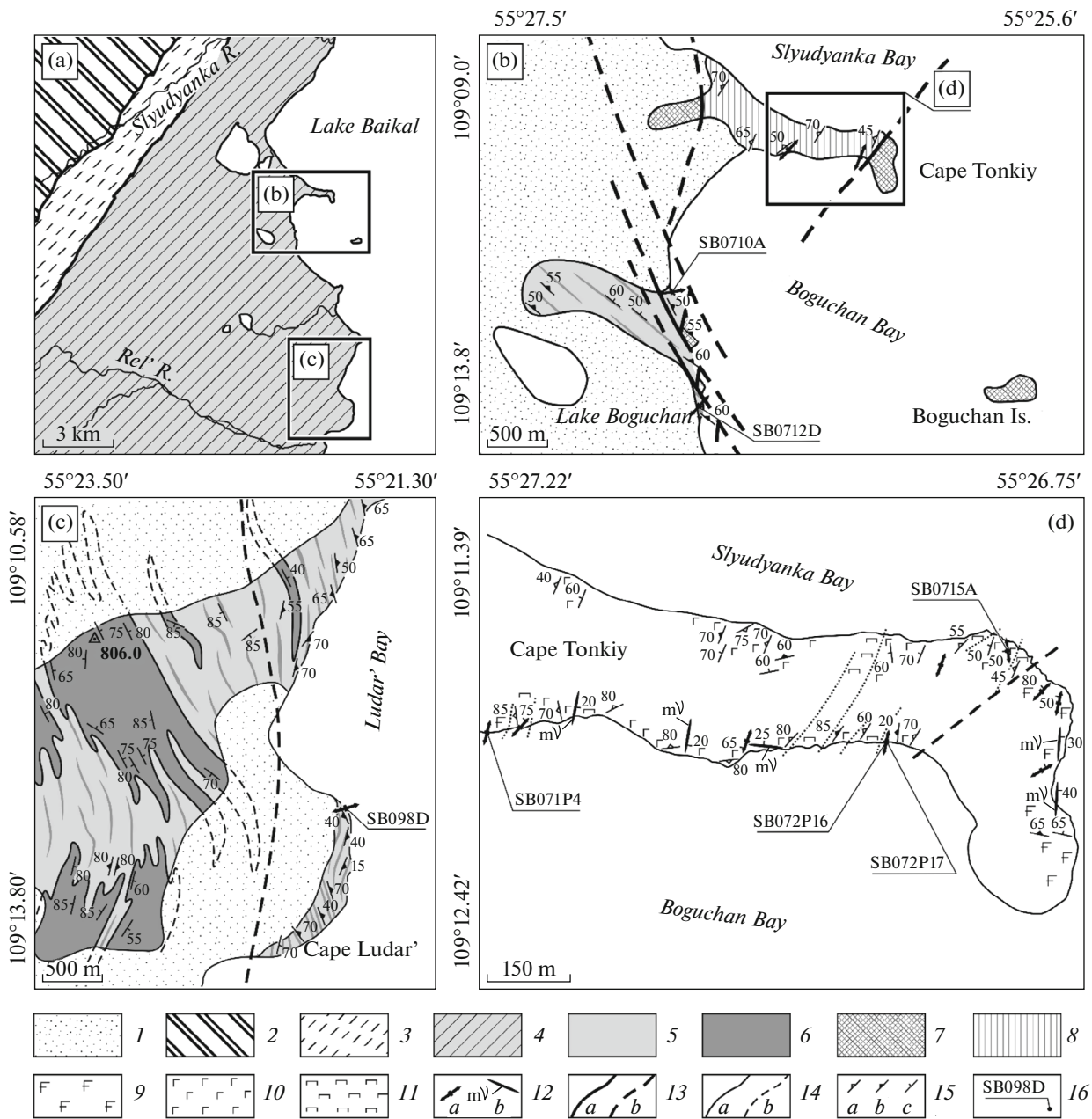


Fig. 3. Geological structure of the western coast of Lake Baikal, between the Slyudyanka and Ludar' bays: (a) a review scheme; (b, c, d) schematic geological map of the Slyudyanka–Rel' interfluvium using data (V.P. Safronov, A.I. Trepalin, V.I. Smolkin et al., 1969), and (Konnikov et al., 1999) modified after (Fedotova et al., 2014). (1) Quaternary undivided sediments (alluvial, proluvial, deluvial, limnic, glacial, and aqueous–glacial): clay, loam, sandy loam, sand, pebble, debris, boulder, blocks; (2) undivided rocks of the Olokit Zone: greenschists, amphibolites, limestone, gneiss; (3) Tectonites: mylonites, blastomylonites; (4–12) Neoproterozoic rocks of the Baikal–Muya Belt: (4) undivided, (5) two-pyroxene crystal schists, amphibolites, amphibolized gabbro; (6) leucocratic crystal schists, enderbites, charnockites; (7) undivided gabbro and amphibole gabbro; (8) undivided gabbro, gabbro-norite, olivine gabbro, troctolite, peridotite, pyroxenite; (9) amphibole gabbro; (10) gabbro, gabbro-norite, olivine gabbro, troctolite; (11) peridotite, pyroxenite; (12) veins and dikes off-scale: (a) complex of granodiorite–leucogranites, rarely garnet plagiogranites, (b) melanogabbro; (13) faults: (a) proved, (b) inferred; (14) geological boundaries: (a) proved, (b) inferred; (15) dip and strike of (a) primary mineral lineation (magmatic), (b) metamorphic banding, (c) contacts of geological bodies, mineral foliation; (16) sampling locality and number.

the northern part of the zone (Mamakan block) comprises ultramafic and mafic rocks and metavolcanics of the Sredne-Mamakan ophiolite complex (Dobretsov et al., 1992; Konnikov et al., 1999; Stanevich and Perelyaev, 1997; Perelyaev, 2003).

The studied Late Neoproterozoic plagiogranite bodies compose (1) small (up to 60 cm thick) vein bodies in the gabbroids of the Sredne-Mamakan ophiolite association; (2) extended dikes up to 40 m thick (traced for no less than 350 m), which cut across dun-

ite–clinopyroxenite–gabbro banded complex of the Sredne-Mamakan ophiolites in the eastern Baikal–Muya belt, as well as 3) tonalite–plagiogranite dikes and vein bodies of the hypabyssal complex of the Kichera zone in the western Baikal–Muya belt. The crystallization age of the granitoid dikes cutting across the Sredne-Mamakan massif constrains the upper age limit of the Sredne-Mamakan ophiolite complex.

During prospecting works, all granitoid massifs developed within the Sredne-Mamakan massif were distinguished as the Early Proterozoic gneiss granites and granites of the Muya Complex (Tikhonov, 1957). Later, these rocks were distinguished as the Early Cambrian (556 ± 16 Ma) Lesnoy Complex (Sryvtsev et al., 1992; Perelyaev, 2003). In the geological maps of new generation, the studied granite bodies are ascribed to the Mesozoic granite porphyry of the Aglan–Yan Complex (Vladimirov and Korobeinikov, 2004).

Plagiogranites dated at 645 ± 10 Ma in the Sredne-Mamakan ophiolite complex of the Karalon–Mamakan zone of the eastern Baikal–Muya belt (Fig. 2) form small veins cutting across leucocratic layered gabbro and are exposed in the upper reaches of the right tributary of the Sredniy Mamakan River (Kröner et al., 2015). These plagiogranite veins are from 15 to 40 cm (sample 2768A) (Table 1) and 60 cm (sample 2774) thick (Table 1), and are spaced near 25 m apart.

The granitoid dikes (samples 2792 and 2793) (Table 1) intruding the dunite–clinopyroxenite–gabbro banded series of the Sredne-Mamakan Complex were studied in the Karalon–Mamakan zone of the eastern Baikal–Muya Belt (Fig. 2). The thickness of the dikes is 35–40 m. They have sharp contacts with rocks of the dunite–pyroxenite–gabbro complex, orienting almost orthogonally to magmatic banding. One sample was dated by U–Pb zircon method (Table 2), while granitoid dikes were studied by Sm–Nd method (Table 3).

The hypabyssal tonalite–plagiogranite complex of the Kichera zone in the western Baikal–Muya belt (Fig. 3) was studied in its best exposed part in the Slyudyanka–Rel' interfluvium. This complex was described in detail in (Fedotova et al., 2014). The granitoids compose series of dikes and morphologically diverse vein bodies, which cut across granulite-facies metamorphic rocks in the northwestern part of Boguchan Bay, alternation of amphibolites and plagiogneisses in the Turkin Brook area, as well as gabbroids of the Kurlin massif, and troctolites and gabbro of the layered complex of Tonkiy Cape. For instance, granitoids intruding the pyroxenite–troctolite–gabbro complex of the Tonkiy Cape massif form small branching veins 1–50 cm thick and relatively extended bodies from 0.3–0.6 to 16–18 m long. The composition and Sm–Nd isotope characteristics of the tonalite–plagiogranite complex were studied in 11 samples of dikes and small vein bodies (Tables 1, 3).

ANALYTICAL METHODS

Concentrations of major components were analyzed by XRF on a S4 Pioneer spectrometer at the Laboratory of Chemical Analytical Studies of the Geological Institute of the Russian Academy of Sciences. Trace elements were analyzed with ICP-MS at the Department of Research–Production Analytical Studies, Institute of Mineralogy, Geochemistry, and Crystal Chemistry of Rare Elements (IMGRE). Samples were prepared for analysis by fusion and microwave decomposition.

Zircon for geochronological studies was extracted from 5-kg plagiogranite sample using a conventional combination of flotation, electromagnetic separation, and heavy liquids at the Laboratory of Chemical Analytical Studies of the Geological Institute of the Russian Academy of Sciences. The plagiogranite sample yielded 200 zircon grains (0.01 g). Isotope-geochronological studies were carried out for size fraction from 70 to 120 μm . Zircon crystals were mounted in epoxy and polished to expose grains. Cathodoluminescence study was conducted on a JEOL JXA-8230 microprobe equipped with a Hamamatsu photonics K.K. PMT R955P panchromatic cathodoluminescent device at the Institute Science de la Terre (ISTerre), Université Grenoble Alpes, Grenoble, France. Images of zircon crystals were obtained at an accelerating voltage of 10 kV and electron current of 7 nA ($\text{nA} = 10^{-9}$ A), counting time of 10 ms. They allowed us to study the internal structure of the grains, which provides insight into zircon origin, and to find undisturbed domains for analytical studies.

Local studies of U–Pb zircon system of tonalites and analysis of Sm–Nd system of granitoids were carried out at the Laboratory of Isotope Geochemistry and Geochronology of the Vernadsky Institute of Geochemistry and Analytical Chemistry of RAS. U–Pb isotope geochronological study of zircon was carried out by LA-ICP-MS on an Element-XR mass spectrometer with ionization in inductively coupled plasma and UP-213 laser system using technique (Kostitsyn and Anosova, 2013). Zircons GJ (Jackson et al., 2004) and 91500 (Weidnbeck et al., 1995) were used as standards. Obtained data were processed using a Glitter software (van Achterbergh et al., 2001). Plotting diagrams with concordia and age calculations using discordia model were carried out using Isoplot software (Ludwig, 2012).

Sm–Nd isotope studies of granitoids were carried out using a conventional technique. Analysis was performed with a 0.03 g aliquot. Samples were digested in hermetically closed vials in HF + HNO₃ mixture in proportions 5 : 1, respectively, on a shaker at IR heating with lamps for three days. After evaporation, a dry residue was washed three times with 1 mL of concentrated HCl with subsequent evaporation. At the first stage, Rb, Sr, and REE fraction were extracted on a fluoroplastic columns with Dowex 50 \times 8 ion

exchange resin by stepwise elution using 2.2 M HCl (for Rb) and 4.0 M HCl (for Sr and REE). Sm and Nd were extracted from REE fraction using Ln-spec columns and a stepwise elution with 0.15, 0.3, and 0.7 M HCl. The concentrations of elements in sample were determined by isotope dilution (Kostitsyn and Zhuravlev, 1987).

Sm-Nd isotope studies were carried out on a multicollector solid phase TRITON mass spectrometer using a double filament ion source. The measurements were carried out in a static mode with simultaneous record of ion currents. The Nd and Sr isotope compositions were corrected by normalization to $^{148}\text{Nd}/^{144}\text{Nd}$ and $^{152}\text{Sm}/^{147}\text{Sm}$, respectively. The technique is reported in detail in (Revyako et al., 2012). Repeated measurements of JNdi-1 standard (Tanaka et al., 2000) yielded $^{143}\text{Nd}/^{144}\text{Nd} = 0.512114 \pm 6$ (2σ ; $N = 10$). The Nd and Sm laboratory blanks are 0.01 and 0.005 ng, respectively. Accuracy of determination of Sm/Nd isotope ratio was estimated at 0.1%.

COMPOSITION OF GRANITOIDS

Granitoid dikes (samples 2792 and 2793) intruding the dunite–pyroxenite–gabbro banded complex of the Sredne-Mamakan massif of the ophiolite association are light gray medium-grained rocks, which in composition correspond to tonalites and leucoplagiogrinites consisting of quartz, altered plagioclase (25–30%), and biotite (up to 10%). K-feldspar, epidote, and clinopyroxene occur in subordinate amounts (near 10%). Accessory minerals are apatite and zircon. Tonalites and plagiogrinites are low-potassium ($\text{K}_2\text{O} < 1.1$ wt %), high-alumina (Al_2O_3 from 14.9 to 18.3 wt %) rocks (Table 1, Fig. 4).

Multielement diagrams show a positive Sr anomaly and negative Nb and Ti anomalies (Fig. 5a). Important geochemical features of the studied rocks are the high Sr content (487–679 ppm), low contents of HREE, Y (<3.4 ppm) and Yb (up to 0.4 ppm) at LREE up to 11 ppm La, and, correspondingly, Sr/Y ratio of (142–309). Such features are typical of granitoids with adakitic geochemical affinity (Defant and Drummond, 1990; Martin, 2005). The REE pattern is differentiated ($(\text{La}/\text{Lu})_N = (17.7–18.5)$, at $\text{Yb}_N = 2.2–2.5$, with a positive Eu anomaly $\text{Eu}/\text{Eu}^* = 1.7–1.8$ (Fig. 5b).

Plagiogrinites forming veins in leucocratic graboids of the Sredne-Mamakan ophiolite complex (2768A and 2774) are light gray medium-grained rocks corresponding to leucoplagiogrinites (73 and 74 wt % SiO_2). They consist of plagioclase (55–60%) partially replaced by sericite, quartz (30–35%), and actinolite (up to 10%). Accessory minerals are apatite and zircon. The plagiogrinites are ascribed to the low-potassium high-alumina ($\text{Al}_2\text{O}_3 = 14.8–14.9$ wt %) rocks (Table 1, Fig. 4). REE distribution pattern is strongly fractionated, with LREE and MREE predominance

over HREE at $(\text{La}/\text{Lu})_N = (23.2–28.5)$, $\text{Yb}_N = 2.5–4.2$, and negative Eu anomaly $\text{Eu}/\text{Eu}^* = 0.6–0.9$ (Fig. 5b). Multielement diagrams show positive Th, U, and Zr anomalies and negative Sr, Nb, and Ti anomalies (Fig. 5a).

Composition of granitoid dikes in the Kichera zone of the western Baikal–Muya Belt is exemplified by the rocks of the hypabyssal complex of the Slyudyanka–Rel’ interfluvial and adjacent territory (Figs. 1, 3), including veins cutting across amphibolite–plagiogneiss complex in the Turkin Brook valley. They are compared with tonalites and plagiogrinites (Konnikov et al., 1999). Hypabyssal complex is dominated by plagiogrinites (65–71 wt % SiO_2), with less common plagioleucogrinites (71–72.5 wt % SiO_2) and leucogrinites (74–75 wt % SiO_2) (Table 1, Fig. 4).

The leucogrinites (SB072R16, 2962, and SB098D) and plagiogrinites SB0712G have a well expressed porphyritic texture, with feldspar phenocrysts up to 2.5 cm in size. Other samples have medium-grained texture without visible phenocrysts. Mafic minerals are mainly represented by pyroxene, with variable proportions of phlogopite and biotite. There are also secondary epidote and amphibole (about 10%). All samples contain quartz–plagioclase intergrowths. Accessory minerals are apatite and zircon.

In the Harker variation diagrams (Fig. 4), the granitoids of the hypabyssal complex define common trends with granitoids of the Kichera Zone (Konnikov et al., 1999) in the western Baikal–Muya belt. Data points of the plagiogrinites of the Sredne-Mamakan ophiolite complex and granitoid dikes cutting across the massif also fall on these trends.

Tonalites (SB072R17), plagiogrinites (SB0712G and 2965), and leucoplagiogrinites (SB0715A and 2810) have high contents of $\text{Al}_2\text{O}_3 = 15.7–20.5$, $\text{Na}_2\text{O} = 3.9–6.3$ (Table 1, Fig. 4). Based on $\text{Sr} = 398–582$, $\text{Y} = 4.3–4.4$ ppm and $\text{Sr}/\text{Y} = 91–136$, the tonalites (SB072R17) and plagiogrinites (SB0712G and 2965) of the dike complex correspond to the granitoids with adakitic geochemical characteristics (Drummond and Defant, 1990; Castillo, 2006) (Table 1, Fig. 5a). These granitoids of the hypabyssal complex of the Kichera Zone, western Baikal–Muya Belt, have a differentiated REE pattern (Fig. 5b), with LREE and MREE predominance over HREE at $(\text{La}/\text{Lu})_N = (13.0–14.0)$, $\text{Yb}_N = 3.1–3.4$, $\text{Eu}/\text{Eu}^* = 1.1–1.2$.

Leucogrinites and granites ascribed to the same complex based on geological data (Fedotova et al., 2014) (dike bodies (SB098D, SB0710A, SB071P4, and SB072P16), as well as vein leucogrinites (2963) and gneissic leucogrinites (2962) alternating with amphibolites demonstrate slightly lower Al_2O_3 content (13.5–16.7 wt %), relatively high Na_2O (3.3–4.3 wt %), and wider range of $\text{K}_2\text{O}/\text{Na}_2\text{O}$ (0.2–1.4) compared to tonalites, plagiogrinites, and leucoplagiogrinites (samples SB072R17, SB0712G, 2965, SB0715A, and

Table 1. Contents of major oxides (wt %) and trace elements (ppm) in (1) granitoid dikes and veins of the Kichera zone in the western Baikal–Muya belt; (2) plagiogranite dikes cutting across dunite–pyroxenite–gabbroic banded series of the Sredne-Mamakan ophiolite complex of the eastern Baikal–Muya belt; (3) plagiogranites of the Sredne-Mamakan ophiolite complex

Component	Group															
	1										2			3		
	2963	SB0715A	2962	2810	SB072R16	SB071R4	SB0710A	SB098D	2965	SB0712G	SB072R17	2793	2792	2768A	2774	
SiO ₂	75.16	74.69	74.51	74.15	73.91	72.49	71.90	71.15	70.88	68.44	65.01	74.10	67.63	73.99	72.57	
TiO ₂	0.05	0.05	0.06	0.02	0.15	0.20	0.18	0.34	0.09	0.38	0.43	0.10	0.27	0.16	0.21	
Al ₂ O ₃	14.50	15.70	14.50	17.12	13.50	13.82	15.24	13.87	20.46	15.70	16.90	14.87	18.31	14.83	14.92	
Fe ₂ O ₃	1.17	0.54	0.41	0.09	0.87	1.94	1.68	2.82	0.32	3.24	3.08	0.89	2.15	1.06	1.31	
MnO	0.02	0.02	0.01	0.05	0.03	0.06	0.03	0.03	0.01	0.04	0.05	0.02	0.03	0.01	0.02	
MgO	0.09	0.10	0.07	0.10	0.80	0.60	0.68	1.06	0.10	1.69	2.55	0.35	0.85	0.41	0.60	
CaO	0.93	0.48	0.87	1.34	1.93	2.11	2.80	2.45	1.07	5.16	5.03	1.73	2.71	1.08	0.77	
Na ₂ O	4.13	7.93	3.80	5.64	4.03	4.21	4.25	3.26	6.31	3.90	4.76	6.08	5.67	6.29	7.39	
K ₂ O	3.60	0.18	4.99	1.15	3.53	2.82	2.79	4.49	0.19	0.71	0.98	1.06	0.84	1.03	0.78	
P ₂ O ₅	0.01	0.02	0.03	0.025	0.07	0.07	0.06	0.09	0.072	0.10	0.15	H.O.	0.11	H.O.	0.04	
L.O.I.	0.34	0.48	0.53	0.27	0.35	0.74	0.40	0.46	0.42	0.65	1.06	0.92	1.44	0.96	0.79	
Total	99.99	100.17	99.77	99.95	99.15	99.03	99.94	99.89	99.92	99.92	99.83	100.09	99.88	99.81	99.40	
Be	–	–	–	–	1.35	0.696	0.849	1.10	–	0.979	0.886	1.35	1.4	2.32	2.58	
V	–	–	–	–	5.79	4.64	6.31	24.9	–	36.4	40.1	6.84	–	18.3	15.3	
Cr	–	–	–	–	41.4	25.5	31.6	34.6	–	24.8	42.8	18.9	–	9.36	11.6	
Mn	–	–	–	–	216	410	133	201	–	236	331	87.6	–	110	108	
Co	–	–	–	–	1.22	2.01	1.55	4.16	–	6.76	9.49	1.64	–	2.20	2.14	
Zn	–	–	–	–	12.2	31.6	11.1	24.7	–	32.7	44.4	6.54	–	36.0	12.5	
Ga	–	–	–	–	15.1	17.1	17.0	13.1	–	17.8	18.2	16.4	17.9	19.9	20.3	
Rb	–	–	–	–	23.9	21.4	15.7	68.5	–	10.3	11.8	15.2	18.5	35.8	21.0	
Sr	–	–	–	–	265	274	190	337	–	398	582	487	679	214	180	
Y	–	–	–	–	6.83	6.66	3.57	6.41	–	4.36	4.28	3.42	2.2	4.29	7.24	
Zr	–	–	–	–	26	122	138	161	–	65	64	122	100	113	182	
Hf	–	–	–	–	0.90	3.37	3.07	3.39	–	1.36	1.52	3.24	2.4	3.56	4.93	
Nb	–	–	–	–	2.55	6.04	2.72	2.05	–	1.25	1.77	2.04	1.05	6.65	11.6	

Table 1. (Contd.)

Component	Group														
	1							2							3
2963	SB0715A	2962	2810	SB072R16	SB071R4	SB0710A	SB098D	2965	SB0712G	SB072R17	2793	2792	2768A	2774	
Cs	—	—	—	0.19	0.09	0.12	0.35	—	0.23	0.07	0.19	0.66	1.54	0.41	
Ba	—	—	—	1116	881	304	1285	—	191	309	769	—	548	368	
La	—	—	—	4.16	23.9	33.1	14.1	—	9.23	8.57	11.1	10.6	16.8	28.9	
Ce	—	—	—	8.65	47.4	65.4	44.5	—	17.3	17.8	20.1	19	29.7	57.4	
Pr	—	—	—	0.93	4.95	7.15	2.73	—	2.03	1.99	1.97	2.10	2.64	5.09	
Nd	—	—	—	3.56	17.30	25.30	8.87	—	7.71	7.68	6.62	7.5	8.42	15.80	
Sm	—	—	—	0.86	2.79	3.81	1.51	—	1.45	1.54	1.10	1.2	1.02	2.44	
Eu	—	—	—	0.43	0.77	1.24	0.58	—	0.45	0.56	0.55	0.59	0.29	0.39	
Gd	—	—	—	0.88	1.86	2.07	1.25	—	1.15	1.26	0.82	0.94	0.92	1.56	
Tb	—	—	—	0.17	0.25	0.21	0.19	—	0.16	0.16	0.11	0.10	0.12	0.22	
Dy	—	—	—	1.08	1.32	0.88	1.06	—	0.84	0.87	0.56	0.46	0.70	1.25	
Ho	—	—	—	0.24	0.26	0.15	0.24	—	0.17	0.16	0.12	0.08	0.13	0.24	
Er	—	—	—	0.71	0.71	0.41	0.82	—	0.42	0.43	0.36	0.23	0.44	0.68	
Tm	—	—	—	0.13	0.11	0.06	0.14	—	0.06	0.06	0.06	0.03	0.05	0.11	
Yb	—	—	—	0.88	0.76	0.43	0.99	—	0.40	0.42	0.38	0.24	0.46	0.69	
Lu	—	—	—	0.15	0.14	0.09	0.19	—	0.07	0.07	0.06	0.06	0.08	0.11	
Ta	—	—	—	0.805	0.278	0.091	0.153	—	0.200	0.318	0.138	—	0.591	0.850	
Th	—	—	—	0.8	1.5	2.1	9.0	—	1.2	1.1	3.8	3.6	13.2	10.9	
U	—	—	—	0.30	0.28	0.17	0.86	—	0.31	0.39	0.90	0.48	2.82	1.75	
Str/Y	—	—	—	38.8	41.1	53.2	52.6	—	91.3	136.0	142.4	308.6	49.9	24.9	
(La/Lu) _N	—	—	—	3.0	17.7	39.4	7.8	—	14.0	13.0	18.5	17.7	23.2	28.5	
Yb _N	—	—	—	2.4	5.0	5.6	3.4	—	3.1	3.4	2.2	2.5	2.5	4.2	
Eu/Eu*	—	—	—	1.5	1.0	1.3	1.3	—	1.1	1.2	1.8	1.7	0.9	0.6	

(SB072P17) tonalite, (SB071P4, SB0712G, SB0710A, 2965) plagiogranites, (SB098D) granite, (SB0715A, 2810) leucoplagiogranites, (SB072P16, 2962) gneissic leucogranites; (2963) leucogranites. Data on samples SB072R17, SB0712G are partially taken after (Fedotova et al., 2014), on samples 2768A and 2774, from (Kröner et al., 2015). Dash means components were not determined, n.d. not detected. Total iron content as Fe₂O₃.

Table 2. Results of U–Pb isotope zircon study (LA-ICP-MS) of tonalite dike cutting across the Sredne-Mamakan ophiolite complex (sample 2792)

Point number	Concentrations		Th/U	Isotope ratios						Rho	Age (Ma)		D, %
	Th, ppm	U, ppm		²⁰⁷ Pb/ ²⁰⁶ Pb	±1σ	²⁰⁷ Pb/ ²³⁵ U	±1σ	²⁰⁶ Pb/ ²³⁸ U	±1σ		²⁰⁶ Pb/ ²³⁸ U	±2σ	
I-01	1013	2497	0.41	0.0609	0.0007	0.861	0.013	0.1026	0.0014	0.70	629.9	16.5	-0.1
I-02	349	1205	0.29	0.0616	0.0007	0.869	0.013	0.1024	0.0014	0.70	628.5	16.1	-1.0
I-04	1474	2472	0.60	0.0635	0.0008	0.926	0.014	0.1058	0.0014	0.70	648.2	16.7	-2.6
I-08	431	1950	0.22	0.0625	0.0007	0.872	0.012	0.1013	0.0013	0.71	621.9	15.8	-2.3
I-09	1448	2149	0.67	0.0624	0.0009	0.916	0.015	0.1065	0.0015	0.69	652.4	17.3	-1.2
I-10	1940	4842	0.40	0.0618	0.0008	0.924	0.015	0.1084	0.0015	0.69	663.8	17.5	-0.1
I-12	107	291	0.37	0.0645	0.0015	0.896	0.022	0.1008	0.0016	0.64	619.3	18.2	-4.7
I-14	175	483	0.36	0.0623	0.0007	0.862	0.012	0.1004	0.0013	0.70	617.0	15.0	-2.3
I-15	2763	3770	0.73	0.0635	0.0007	0.923	0.013	0.1055	0.0014	0.70	646.4	15.9	-2.6
I-17	521	1321	0.39	0.0616	0.0007	0.873	0.013	0.1029	0.0014	0.70	631.5	16.1	-0.9
I-18	191	194	0.98	0.0624	0.0008	0.892	0.013	0.1037	0.0014	0.69	636.4	15.8	-1.8
I-19-1	476	1894	0.25	0.0615	0.0009	0.888	0.016	0.1048	0.0015	0.69	642.4	17.6	-0.4
I-19-2	481	1980	0.24	0.0611	0.0009	0.884	0.015	0.1049	0.0015	0.69	643.4	17.2	0.1
I-20	485	340	1.42	0.0635	0.0008	0.885	0.014	0.1011	0.0014	0.69	620.8	15.8	-3.6
II-01	29	111	0.26	0.0604	0.0009	0.840	0.012	0.1009	0.0010	0.62	619.9	12.0	0.1
II-04	293	756	0.39	0.0614	0.0007	0.852	0.010	0.1007	0.0010	0.64	618.6	11.4	-1.2
II-05	190	417	0.46	0.0626	0.0008	0.853	0.010	0.0987	0.0010	0.64	607.2	11.3	-3.0
II-10	744	1895	0.39	0.0636	0.0008	0.857	0.010	0.0977	0.0010	0.65	600.8	11.6	-4.4
II-12	297	705	0.42	0.0614	0.0007	0.862	0.010	0.1018	0.0010	0.65	624.9	11.6	-1.0
II-14-1	254	517	0.49	0.0626	0.0007	0.842	0.009	0.0976	0.0010	0.65	600.7	11.2	-3.2
II-14-2	277	526	0.53	0.0614	0.0007	0.834	0.011	0.0986	0.0012	0.70	606.4	14.6	-1.6
II-15	109	327	0.33	0.0620	0.0008	0.846	0.010	0.0990	0.0010	0.64	608.5	11.3	-2.2
II-16	97	333	0.29	0.0609	0.0007	0.858	0.010	0.1022	0.0010	0.64	627.4	11.7	-0.3
II-17-1	307	625	0.49	0.0663	0.0008	0.922	0.013	0.1008	0.0013	0.69	619.2	14.8	-6.7
II-17-2	1117	1657	0.67	0.0633	0.0007	0.890	0.010	0.1018	0.0010	0.65	625.1	11.9	-3.3
II-18-1	297	303	0.98	0.0605	0.0009	0.915	0.013	0.1096	0.0011	0.63	670.5	13.2	1.6
II-18-2	396	312	1.27	0.0622	0.0007	0.859	0.012	0.1002	0.0013	0.70	615.7	14.8	-2.2
II-19	501	1327	0.38	0.0607	0.0007	0.857	0.009	0.1023	0.0010	0.65	628.2	11.7	0.0
II-20-1	438	1018	0.43	0.0610	0.0007	0.824	0.011	0.0979	0.0013	0.70	602.4	14.7	-1.2
II-20-2	589	1288	0.46	0.0608	0.0008	0.905	0.011	0.1079	0.0011	0.65	660.8	12.9	0.9
III-01	223	847	0.26	0.0628	0.0012	0.868	0.018	0.1002	0.0013	0.63	615.9	14.8	-2.9
III-03	377	454	0.83	0.0617	0.0011	0.886	0.016	0.1041	0.0012	0.63	638.6	14.2	-0.9
III-04	744	1900	0.39	0.0639	0.0008	0.971	0.014	0.1102	0.0013	0.66	674.0	15.0	-2.2
III-05	216	676	0.32	0.0607	0.0007	0.855	0.012	0.1022	0.0013	0.70	627.2	15.7	-0.1
III-08-1	101	231	0.44	0.0603	0.0008	0.861	0.013	0.1035	0.0013	0.68	635.1	15.5	0.7
III-08-2	457	1436	0.32	0.0632	0.0008	0.903	0.012	0.1036	0.0011	0.65	635.6	13.0	-2.7
III-09-1	308	875	0.35	0.0612	0.0007	0.848	0.012	0.1005	0.0013	0.70	617.4	15.4	-1.0
III-09-2	931	1912	0.49	0.0613	0.0008	0.903	0.012	0.1067	0.0012	0.67	653.5	14.4	0.0
III-11-1	645	698	0.92	0.0623	0.0008	0.889	0.013	0.1035	0.0014	0.69	635.1	16.3	-1.7
III-11-2	295	926	0.32	0.0624	0.0008	0.891	0.012	0.1036	0.0011	0.65	635.4	13.4	-1.7
III-12	77	212	0.36	0.0618	0.0009	0.871	0.013	0.1022	0.0012	0.64	627.4	13.5	-1.4

Table 2. (Contd.)

Point number	Concentrations		Th/U	Isotope ratios						Rho	Age (Ma)		D, %
	Th, ppm	U, ppm		$^{207}\text{Pb}/^{206}\text{Pb}$	$\pm 1\sigma$	$^{207}\text{Pb}/^{235}\text{U}$	$\pm 1\sigma$	$^{206}\text{Pb}/^{238}\text{U}$	$\pm 1\sigma$		$^{206}\text{Pb}/^{238}\text{U}$	$\pm 2\sigma$	
III-14	78	391	0.20	0.0627	0.0008	0.911	0.014	0.1054	0.0014	0.69	646.2	16.3	-1.7
III-15	52	114	0.46	0.0637	0.0011	0.909	0.015	0.1034	0.0012	0.63	634.4	13.8	-3.4
III-16-1	40	48	0.82	0.0639	0.0014	0.905	0.020	0.1028	0.0012	0.61	631.1	14.2	-3.6
III-16-2	47	63	0.75	0.0612	0.0010	0.844	0.014	0.1001	0.0013	0.65	614.9	14.8	-1.0
III-18	146	445	0.33	0.0614	0.0008	0.846	0.013	0.0999	0.0013	0.69	614.2	15.5	-1.3
III-19-1	56	161	0.35	0.0623	0.0009	0.866	0.014	0.1008	0.0013	0.68	619.2	15.7	-2.2
III-19-2	252	382	0.66	0.0647	0.0008	0.915	0.012	0.1025	0.0011	0.65	629.2	12.8	-4.6
III-22	1642	3191	0.51	0.0616	0.0007	0.832	0.012	0.0981	0.0013	0.71	603.2	15.4	-1.9
III-23-1	229	420	0.55	0.0608	0.0008	0.858	0.014	0.1023	0.0014	0.69	627.9	16.3	-0.2
III-23-2	226	497	0.45	0.0638	0.0008	0.899	0.011	0.1021	0.0011	0.66	627.0	12.8	-3.7
III-27	232	1141	0.20	0.0613	0.0008	0.862	0.014	0.1020	0.0014	0.70	626.2	16.6	-0.8
III-29	104	306	0.34	0.0860	0.0010	1.233	0.017	0.1040	0.0013	0.70	638.0	15.2	-21.8
III-30-1	191	284	0.67	0.0614	0.0009	0.886	0.013	0.1045	0.0012	0.64	640.7	14.0	-0.5
III-30-2	196	285	0.69	0.0615	0.0008	0.879	0.014	0.1037	0.0014	0.69	636.3	16.5	-0.7
III-31	239	601	0.40	0.0610	0.0008	0.860	0.013	0.1024	0.0014	0.70	628.5	16.4	-0.3
III-32	235	366	0.64	0.0605	0.0008	0.905	0.014	0.1085	0.0014	0.69	664.1	16.6	1.5
III-37	244	985	0.25	0.0624	0.0009	0.936	0.013	0.1089	0.0012	0.64	666.5	14.0	-0.7
III-38	390	912	0.43	0.0619	0.0008	0.875	0.013	0.1025	0.0014	0.70	629.3	16.5	-1.4
III-46-1	322	274	1.18	0.0627	0.0009	0.868	0.012	0.1005	0.0011	0.64	617.2	12.6	-2.8
III-46-2	110	592	0.19	0.0608	0.0008	0.849	0.013	0.1013	0.0014	0.69	622.3	16.1	-0.3
III-47-1	226	276	0.82	0.0617	0.0008	0.854	0.013	0.1005	0.0013	0.70	617.2	15.8	-1.6
III-47-2	302	313	0.96	0.0631	0.0010	0.859	0.014	0.0986	0.0011	0.63	606.3	13.2	-3.7
III-48	322	319	1.01	0.0618	0.0008	0.886	0.012	0.1039	0.0011	0.64	637.2	12.9	-1.1
III-49	224	255	0.88	0.0603	0.0008	0.854	0.014	0.1027	0.0014	0.69	630.1	16.3	0.5

Rho—is the correlation coefficient in error of $^{207}\text{Pb}/^{235}\text{U}$ and $^{206}\text{Pb}/^{238}\text{U}$ ratios; D is the degree of discordance.

Table 3. Sm–Nd isotope data on the granitoids of the Kichera zone, western Baikal–Muya belt (1); plagiogranite dikes intersecting the rocks of the dunite–pyroxenite–gabbroic layered series of the Sredne-Mamokan ophiolite complex of the eastern Baikal–Muya Belt (2) and plagiogranites from the Sredne-Mamokan ophiolite complex (3)

Sample	Group	Sm	Nd	$^{147}\text{Sm}/^{144}\text{Nd}$	$^{143}\text{Nd}/^{144}\text{Nd} \pm 2\sigma$	$\epsilon_{\text{Nd}}(\text{T}) \pm 2\sigma$	$T_{\text{Nd}}(\text{DM}),$ Ga
2963	1	0.54	1.97	0.1654	0.512818 ± 25	$+5.9 \pm 0.3$	0.92
2962		1.27	5.82	0.1319	0.512575 ± 04	$+3.8 \pm 0.1$	1.00
SB072R16		2.43	16.68	0.0879	0.512554 ± 19	$+6.7 \pm 0.5$	0.67
SB098D		1.42	8.51	0.1013	0.512428 ± 09	$+3.2 \pm 0.3$	0.92
2965		1.45	6.92	0.127	0.512711 ± 20	$+6.8 \pm 0.5$	0.70
SB0712G		0.92	4.82	0.1153	0.512556 ± 13	$+4.7 \pm 0.3$	0.86
SB072R17		1.72	9.5	0.1093	0.512657 ± 17	$+7.1 \pm 0.4$	0.66
2793	2	1.34	8.07	0.1004	0.512388 ± 04	$+2.5 \pm 0.1$	0.97
2792		1.12	6.77	0.1004	0.512466 ± 06	$+4 \pm 0.1$	0.87
2768A	3	1.48	10.8	0.0831	0.512145 ± 11	-0.9 ± 0.2	1.13
2774		1.47	8.52	0.1046	0.512209 ± 12	-1.3 ± 0.2	1.26

Model parameters: chondrite uniform reservoir (CHUR) $^{143}\text{Nd}/^{144}\text{Nd} = 0.512638$, $^{147}\text{Sm}/^{144}\text{Nd} = 0.1967$; depleted mantle reservoir (DM) $^{143}\text{Nd}/^{144}\text{Nd} = 0.513099$, $^{147}\text{Sm}/^{144}\text{Nd} = 0.2119$. T = 600 Ma.

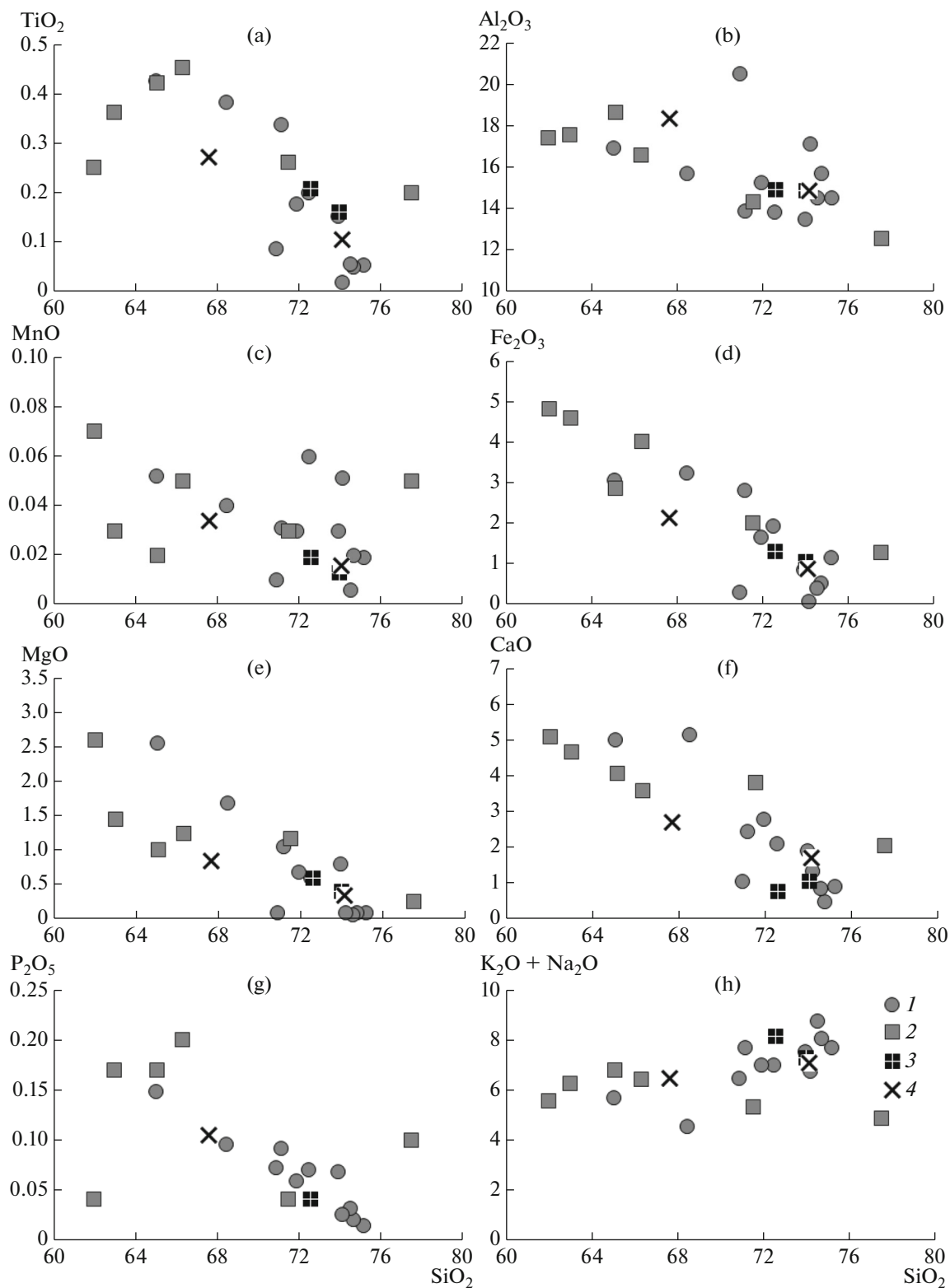


Fig. 4. Harker diagrams for (1) granitoids from dikes and veins of the Kichera zone, western Baikal–Muya belt (this work), (2) granitoids from dikes and veins of the Kichera zone, western Baikal–Muya belt (Konnikov et al., 1999); (3) plagiogranites from the Sredne-Mamakan ophiolite complex of the eastern Baikal–Muya Belt; (4) tonalities and plagiogranite from dikes cutting across the rocks of the Sredne-Mamakan massif of the eastern Baikal–Muya Belt.

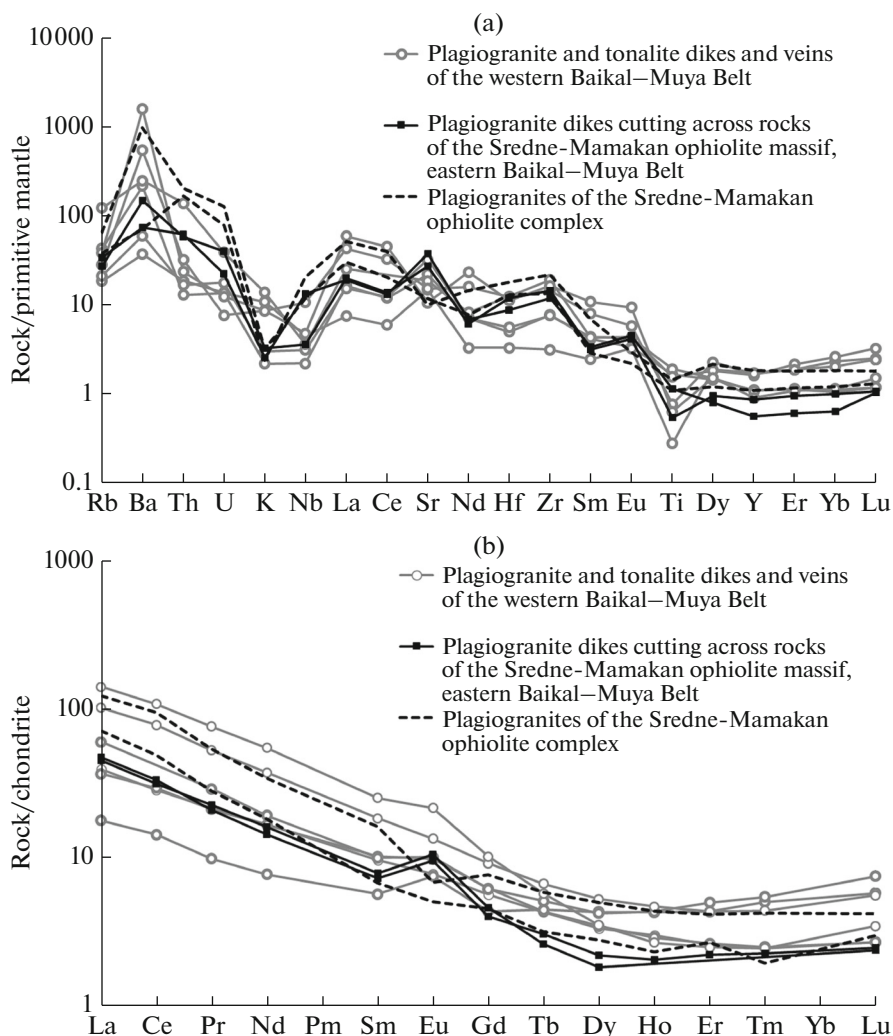


Fig. 5. (a) Multi-element diagrams for granitoids of the western Baikál–Muya Belt from (Fedotova et al., 2014); for plagiogranite from the ophiolite complex of the eastern Baikál–Muya Belt (sample 2774) and for plagiogranite dikes cutting across the rocks of the Sredne-Mamakan massif (samples 2792 and 2793). Composition of primitive mantle after (Taylor and McLennan, 1985). (b) REE distribution pattern for cross-cutting granitoids in the western Baikál–Muya Belt; for plagiogranite from ophiolite complex of the eastern Baikál–Muya Belt (sample 2774) and for plagiogranite dikes cutting across the rocks of the Sredne-Mamakan massif (samples 2792 and 2793). Chondrite composition after (Sun & McDonough, 1989).

2810) (Table 1, Fig. 4). The rocks have lower Sr content, but sufficiently high Sr/Y ratio (39–53). The REE distribution patterns of the leucogranites SB072P16 and plagiogranites SB098D are less differentiated, show LREE and MREE predominance over HREE at $(La/Lu)_N = (3.0–7.8)$, $Yb_N = 2.4–3.4$, $Eu/Eu^* = 1.3–1.5$. The plagiogranites SB071P4 and SB0710A have strongly differentiated pattern, LREE and MREE predominance over HREE, at $(La/Lu)_N = (17.7–39.4)$, $Yb_N = 5.0–5.6$, $Eu/Eu^* = 1.0–1.3$ (Table 1, Fig. 5b).

Thus, based on geochemical features, some of the studied granitoids from the western part and plagiogranites from the eastern part of the Baikál–Muya Belt are ascribed to adakites, the rocks with fractionated REE pattern, low HREE and Y contents, and high Sr contents (Fig. 5).

In composition, they sharply differ from plagiogranites forming veins up to 60 cm thick in the leucocratic gabbroids of the Sredne-Mamakan ophiolite complex. The presence of negative Eu and Sr anomalies and elevated Th and Nb suggest that a source of these rocks differed from those of two other associations (Fig. 5, Table 1). Specifics of the plagiogranite veins from ophiolite complex could reflect the crystallization differentiation of parental mafic magma.

RESULTS OF ISOTOPE STUDIES

Zircon from plagiogranites intersecting the dunite–pyroxene–gabbro banded series of the Sredne-Mamakan ophiolite complex (Fig. 2, sample 2792) is represented by two morphological types: elongated-prismatic (up to acicular) grains with smoothed facets

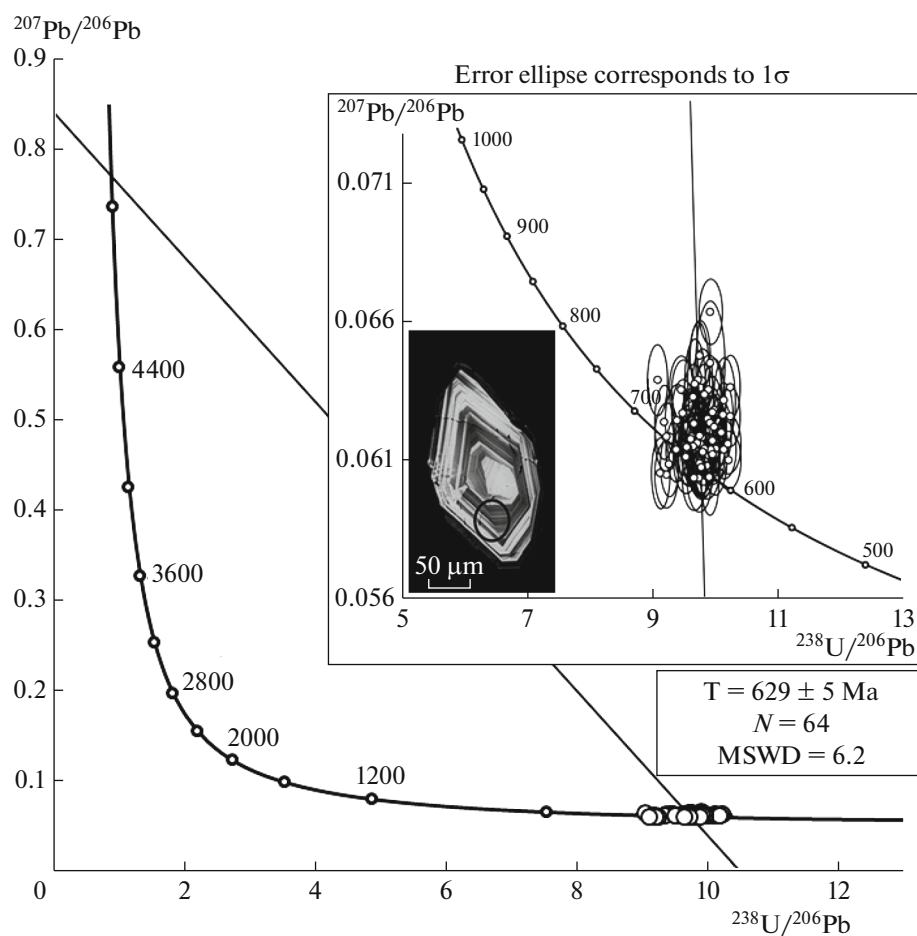


Fig. 6. U–Pb data in the Terra–Wasserburg diagram for zircon from plagiogranite dikes (sample 2792) intersecting the rocks of the Sredne-Mamakan massif. Inset shows the same plot in a magnified scale. Age was calculated from 64 points, and solid lines show the error ellipses. Figure presents the cathodoluminescence image of typical magmatic zircon from plagiogranite sample 2792. Circle in zircon crystal shows the laser beam diameter during local analysis.

and apexes (elongation ratio of 1 : 3–1 : 6) and short-prismatic grains with smoothed pyramida facets and partially preserved prisma facets. Crystals are mainly fractured, transparent, and translucent, yellowish, light brown. Cathodoluminescence images of the zircon show oscillatory (thin concentric) zoning, as well as inclusions, fractures, metamict zones, and other disturbances. The analyses were made for most transparent and nonfractured grains devoid of inclusions.

U–Pb isotope data on 54 zircon grains from plagiogranites were used to plot diagram with concordia. Eleven crystals were analyzed in two zones, but the age values and Th and U concentrations in the inner and outer zones of zircon are overlapped within error (Table 2). We may conclude that the studied grains do not contain ancient cores. This is consistent with results of cathodoluminescent study of zircon (Fig. 6).

The studies were carried out in 65 points, some of which are discordant (Table 2). It is seen in the Terra–Wasserburg diagram (Fig. 6) that data points plot near concordia, but some of them deviate along discordia

intersecting with y -axis at $^{207}\text{Pb}/^{206}\text{Pb} = 0.84$, which corresponds to the composition of modern lead. It is probable that many zircon grains contain admixture of common lead (Kostitsyn and Anosova, 2013). One composition point (III-29) was excluded from age calculations due to strong discordance ($D = -22\%$) (Table 2). As a result, 64 points yielded the upper intercept age of 629 ± 5 Ma. The morphology and thin concentric zoning (Fig. 6), suggest a magmatic origin of the zircon. Hence, the obtained age value is the crystallization age of the plagiogranite dikes cutting across the dunite–pyroxenite–gabbro banded series of the Sredne-Mamakan ophiolite association.

In all studied granitoid varies, we analyzed Nd and Sm isotope ratios, calculated $\epsilon_{\text{Nd}}(T)$ for an age of 600 Ma, and model ages $T_{\text{Nd}}(\text{DM})$. Results of Sm–Nd isotope studies are listed in Table 3.

Plagiogranites from the Sredne-Mamakan ophiolite complex (samples 2768A and 2774) have Sm = 1.47–1.48 and Nd = 9–11 ppm, $^{147}\text{Sm}/^{144}\text{Nd}$ isotope

ratios of 0.0831 and 0.1046, and $^{143}\text{Nd}/^{144}\text{Nd}$ isotope ratios of 0.512145 and 0.512209, respectively (Table 3). The values of model ages $T_{\text{Nd}}(\text{DM})$ account for 1.13 and 1.26 Ga, and $\epsilon_{\text{Nd}}(\text{T})$ values equal -0.9 and -1.3 , respectively.

Tonalite and plagiogranite (samples 2792 and 2793) dikes intersecting the rocks of the Sredne-Mamakan Complex contain 1.1–1.3 ppm Sm, 7–8 ppm Nd. $^{147}\text{Sm}/^{144}\text{Nd}$ isotope ratios are 0.1004, and $^{143}\text{Nd}/^{144}\text{Nd} = 0.512388$ and 0.512466 , respectively. The values of model age $T_{\text{Nd}}(\text{DM})$ are 0.97 and 0.87 Ga, and $\epsilon_{\text{Nd}}(\text{T})$ are $+2.5$ and $+4.0$, respectively.

The study of Nd isotope composition revealed significant difference between two plagiogranite types, which occupy different positions relative to the Sredne-Mamakan massif (Table 3). The granitoids of the adakite group that were emplaced at 629 ± 5 Ma along fracture system in the rocks of the banded series have $\epsilon_{\text{Nd}}(\text{T}) = +2.5$ and $+4$, whereas the ophiolite type rocks that crystallized at 645 ± 10 Ma have close negative $\epsilon_{\text{Nd}}(\text{T}) = -0.9$ and -1.3 .

The Sm and Nd contents in the granitoid samples of the dike complex and leucocratic gneissic granites of the Kichera Zone of the western Baikal–Muya belt are 0.5–2.4 and 2–17 ppm, respectively. The $^{147}\text{Sm}/^{144}\text{Nd}$ and $^{143}\text{Nd}/^{144}\text{Nd}$ isotope ratios vary from 0.0879 to 0.1654 and from 0.512428 to 0.512818, respectively. The model ages of the dike granitoids from the western part of the belt were determined within 0.66–1.00 Ga. The granitoids have $\epsilon_{\text{Nd}}(\text{T}) = +3.2\dots+7.1$.

The studied rocks of the hypabyssal complex of the Kichera zone, western Baikal–Muya Belt, are subdivided into different types: tonalites and plagiogranites with adakitic geochemical affinity and non-adakitic granites-leucogranites. The model ages $T_{\text{Nd}}(\text{DM})$ of the tonalites (sample SB072P17) and plagiogranites (samples SB0712G and 2965) of the adakite group are 0.66–0.86 Ga. Adakitic tonalites define an U–Pb laser ablation age of 595 ± 5 Ma (Fedotova et al., 2014). These data indicate that the granitoids were produced by partial melting of a protolith with a short crustal residence time. The values of $\epsilon_{\text{Nd}}(\text{T})$ for these samples are $+4.7\dots+7.1$. The model ages of granites (sample SB098D) and leucogranites (samples SB072P16, 2962, and 2963) of non-adakitic group account for 0.67–1.00 Ga. The values of $\epsilon_{\text{Nd}}(\text{T})$ for these rocks are $+3.2\dots+6.7$.

As mentioned above, plagiogranites forming veins in the leucocratic gabbroids of the Sredne-Mamakan ophiolite complex differ from the rocks of two other associations in negative $\epsilon_{\text{Nd}}(\text{T})$ values. It is noteworthy that these plagiogranites have the same Nd isotope composition as host gabbroic rocks (Somsikova et al., 2019). Assuming that both gabbroids and vein plagiogranites were formed in a subduction setting, such Nd parameters suggest the involvement of subducted

sediments or other crustal material in a partial melting zone.

GEOCHEMISTRY AND ISOTOPE COMPOSITION OF THE LATE NEOPROTEROZOIC GRANITOIDS OF THE BAIKAL–MUYA BELT

Obtained data on the granitoids of the Karalon–Mamakan zone in the eastern Baikal–Muya fold belt showed that they have adakitic geochemical characteristics: high-alumina sodic intermediate and felsic rocks with Sr >400 ppm (Sr = 487–679 ppm), low Y < 5 ppm (Y = 2.2–3.4 ppm) and heavy REE, in particular, Y contents < 1 ppm (Yb = 0.2–0.4 ppm) (Table 1). Adakites are formed within a narrow range of conditions and are important indicators of geodynamic reconstructions, which mark episodes of partial melting of mafic crust. Adakitic magmas that are scarce for Late Precambrian and subsequent time and typical of such melting episodes, in composition are similar to magmas that produced tonalite–trondhjemite–granodiorite series of the Archean and Paleoproterozoic crust. Partial melting of mafic protolith, which is frequently reconstructed for Early Precambrian, became a scarce event in the subsequent geological history (Defant and Drummond, 1990).

Positive values of $\epsilon_{\text{Nd}}(\text{T})$ is a peculiar feature of the Late Neoproterozoic granitoids and felsic volcanics of the Baikal–Muya fold belt. Rytsk et al. (2001, 2004, 2007) determined isotope-geochemical features of sources of rhyolites and granitoids of the Karalon–Mamakan zone: $\epsilon_{\text{Nd}}(\text{T}) = +6.4\dots+8.2$ —for dacites and rhyolites of the Yakor’ and Karalon sequences and diorites of the Tallain Complex, $\epsilon_{\text{Nd}}(0.6) = +4.7\dots+5.4$ —for rhyolites and granite porphyry of the Padrin Group, $\epsilon_{\text{Nd}}(0.6) = +3.9$ —for granites of the Lesnoy Complex. The rocks of the Padrin Group are dated at 590 ± 5 Ma (Rytsk et al., 2004), and granites of the Lesnoy Complex, at 556 ± 16 Ma (Srytsev et al., 1992).

Sm–Nd isotope-geochemical characteristics of the studied tonalite and plagiogranite dikes cutting across the dunite–pyroxenite–gabbroic series of the Sredne-Mamakan ophiolite complex from the eastern part of the belt ($\epsilon_{\text{Nd}}(\text{T}) = +2.5; +4.0$), in complex with petrological-geochemical data indicate that the rocks were formed by partial melting of a juvenile Neoproterozoic crust.

The rocks of the dike system cutting across the dunite–pyroxenite–gabbro banded series of the Sredne-Mamakan ophiolite complex are not correlated with previously distinguished granitoid complexes. Based on the geological relations and geochemical features reflecting likely a change of paleogeodynamic setting, the granitoid dikes with adakitic geochemical affinity are ascribed to the earliest post-ophiolite magmatic series. Dikes developed in the

upper reaches of the Dremuchiy Brook (tonalite 2792 and plagiogranite 2793) (Fig. 2, Tables 1–3) could be considered as typical magmatic bodies of independent complex with specific geochemical composition and age of 629 ± 5 Ma (Table 2, Fig. 6).

Relatively low $\epsilon_{Nd}(T) = -0.9; -1.3$ (Table 3) for plagiogranites (as for gabbro of the considered ophiolite complex ($\epsilon_{Nd}(T) = -1.8...+0.2$) (Somsikova et al., 2019)) are likely related to the suprasubduction conditions of the formation of the Sredne-Mamakan ophiolite association (Perelyaev, 2003). Subrasubduction ophiolites are referred to as relicts of oceanic lithosphere of basins formed during extension above subduction zone. Such basins could be situated in back-arc or fore-arc area or are formed by collapse of the volcanic arc.

In other words, the oceanic crust was likely formed during suprasubduction extension according to mechanism considered in (Sklyarov et al., 2016). These conditions provide mixing of mantle and crustal material owing to the contribution of subducted sediments in mantle wedge in compliance with the widely known model or the involvement of sialic material of volcanic arc according to mechanism considered, in particular, in (Taylor and Martinez, 2003). Ophiolite allochthons could contain also separate island-arc nappes with corresponding isotope characteristics (e.g., Pfänder et al., 2002).

The hypabyssal complex of the Kichera zone in the western Baikal–Muya Belt (Figs. 1, 3) also comprises granitoids with geochemical adakitic characteristics (Table 1, Fig. 5). These granitoids have younger age (595 ± 5 Ma) than dike rocks intersecting the rocks of the dunite–pyroxenite–gabbro banded series of the Sredne-Mamakan ophiolite complex (629 ± 5 Ma) and higher positive $\epsilon_{Nd}(T) = +4.7...+7.1$. Variations of Nd isotope composition in the plagiogranites of the Kichera zone are consistent with an inferred heterogeneity of source of the granitoid magmas, which corresponds mainly to the juvenile Neoproterozoic crust. A protolith heterogeneity is confirmed by a wide range of $^{147}\text{Sm}/^{144}\text{Nd}$ values from 0.0879 to 0.1654 (Table 3), as well as rock composition of the considered granitoid series varying from tonalites to leucogranites and mentioned above indicator contents of trace elements and their variations (Table 1, Figs. 4, 5).

The age and Sm–Nd isotope data on the granitoids of the Kichera zone of the western Baikal–Muya belt ($\epsilon_{Nd}(T) = +3.2...+7.1$ (Table 3), crystallization age of 595 ± 5 Ma), and rhyolites and granite porphyry of the Padrin Group ($\epsilon_{Nd}(T) = +4.7...+5.4$, crystallization age of 590 ± 5 Ma (Rytsk et al., 2004)) give grounds to suggest that the rocks have a common origin and that the rhyolites of the Padrin Group of the Karalon–Mamakan zone, eastern Baikal–Muya Belt, could be volcanic analogues of the granitoids of the hypabyssal complex of the Kichera zone, western Baikal–Muya Belt.

SEQUENCE OF GRANITOID MAGMATISM IN THE BAIKAL–MUYA BELT DURING THE LATE NEOPROTEROZOIC

The Baikal–Muya Belt comprises relicts of different marginal-continental Neoproterozoic complexes, which by the end of Neoproterozoic were accreted into fold belt. The Neoproterozoic complexes are represented by metavolcanic rocks and amphibolites, spatially related ultramafic and mafic rocks, high-grade metamorphic rocks, plutonic associations of differentiated gabbro–granite, gabbro, and granitic series, volcanogenic, and volcanosedimentary sequences. Of great importance for deciphering the geological evolution of the Baikal–Muya fold belt are finds and dating of eclogites (Gabov et al., 1984; Shatsky et al., 2012), granulites (Makrygina et al., 1993, 1989; Amelin et al., 2000; Fedotova et al., 2014; Kröner et al., 2015), determination of the nature of mafic–ultramafic complex (ophiolites or intrusive associations) (Makrygina et al., 1993; Izokh et al., 1998; Konnikov et al., 1999; Tsygankov, 2005, and others), and study of detrital material of molasses sequences (Salop, 1964; Stanevich et al., 2007, etc.). Dike granitoids corresponding in composition to adakites (Table 1) are one more marker for the incipient magmatic reworking of the mafic crust, which was likely related to the local break-off of the subducted plate.

Relations between magmatic and metamorphic complexes of the late Neoproterozoic stage and position of adakites in the eastern (Fig. 7a) and western (Fig. 7b) branches of the Baikal–Muya belt are schematically shown in the figures.

The Muya high-grade block with Late Neoproterozoic eclogites is distinguished in the axial part of the eastern Baikal–Muya Belt (Avchenko et al., Shatskii et al., 2014). In the northeast, it is bordered by the Karalon–Mamakan zone, which consists of volcanogenic sequences, components of the ophiolite complex, intrusive series, and sedimentary sequences (Figs. 1, 2). This zone of the eastern Baikal–Muya belt adjoins the Patom terrane of the Neoproterozoic Siberian margin (Fig. 1).

The Late Neoproterozoic intrusion of the Karalon–Mamakan zone (Fig. 7a) in the eastern part of the belt are contained in the island-arc volcanosedimentary Karalon and Yakor' sequences with an age of 664 ± 3 Ma (Rytsk et al., 2001). The granites and rhyolites of the Karalon sequence have high positive $\epsilon_{Nd}(T)$ from +7.1 to 8.2, which indicate the predominant contribution of depleted mantle in a source (Rytsk et al., 2001). The age of the ophiolites of the Sredne-Mamakan Complex of the Baikal–Muya Belt is estimated at 645 ± 10 Ma based on zircon dating of plagiogranites (Kröner et al., 2015), and at $774 \pm 67–704 \pm 71$ Ma based on Sm–Nd isochron dating of rocks of the banded series (Rytsk et al., 2001). Two studied granitoid samples of the ophiolite complex have $\epsilon_{Nd}(T)$ of -0.9 and -1.3 , ($T_{Nd}(DM) = 1.13$ and

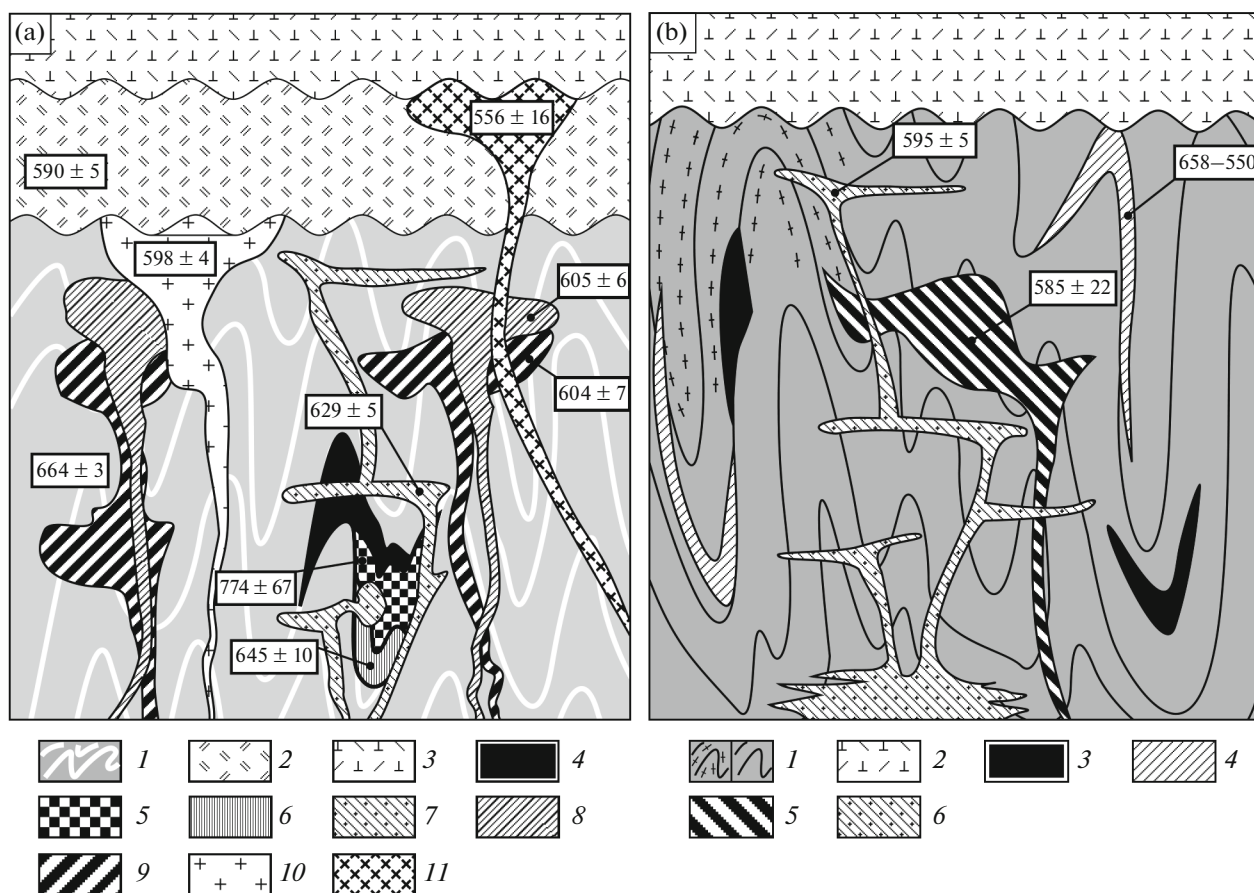


Fig. 7. (a) Schematic emplacement model of the Late Neoproterozoic lithological complexes of the eastern Baikal–Muya volcanoplutonic belt: (1) metavolcanic rocks of the Karalon Sequence, 664 ± 3 Ma, metarhyolites (Rytsk et al., 2001); (2) Padrin volcanoplutonic series, 590 ± 5 Ma, rhyolites (Rytsk et al., 2004); (3) sedimentary sequences of the Mamakan Group, molasses (Yakra, Padrokan, Shumninskaya, and Delyun-Uran sequence), Late Neoproterozoic (Rytsk et al., 2001); (4–6) Sredne-Mamakan ophiolite complex: (4) ultramafic rocks, (5) dunite–pyroxenite–gabbro (gabbronorite) banded complex, 774 ± 7 Ma, rocks from a single rhythm, including leucocratic gabbronorites, 704 ± 71 Ma, leucocratic gabbronorites (both values from (Rytsk et al., 2001), Figure shows the former), (6) leucocratic banded gabbro bearing single dolerite dikes (metadolerites) and plagiogranites, 645 ± 10 Ma (Kröner et al., 2015); (7) postophiolite granitoids with adakitic affinity, 629 ± 5 Ma (this work); (8–9) Tallain gabbro–diorite–plagiogranite complex: (8) 605 ± 6 Ma, diorites and plagiogranites, (9) 604 ± 7 Ma, gabbro and gabbrodorites (Rytsk et al., 2007, 2012); (10) diorites ad granites of the Padrorites, 598 ± 4 Ma, granites (Rytsk et al., 2007a); (11) granitoids of the Lesnoy Complex, 556 ± 16 Ma, granites (Sryvtsev et al., 1992). (b) Schematic model of emplacement of lithological complexes of the western Baikal–Muya volcanoplutonic belt: (1) mainly basaltic rocks of the Nyurundukan Sequence, >640 Ma, and granulites/amphibolites after them, 618 ± 5 enderbites, 640 ± 5 two-pyroxene gneisses (Amelin et al., 2000; Kröner et al., 2015); (2) sedimentary sequences, molasse (Stanevich et al., 2007); (3) ultramafic–mafic rocks; (4) gneissic plagiogranites in the development area of the Nyurundukan Sequence, 658–550 Ma, Muya granites (Neimark et al., 1995); (5) Tonkiy Cape pyroxenite–troctolite–gabbro complex, 585 ± 22 Ma, troctolites (Makrygina et al., 1993); (6) granitoids with geochemical characteristics of adakites and plagiomigmatites of similar composition (Konnikov et al., 1999), 595 ± 5 Ma (Fedotova et al., 2014).

1.26 Ga), while gabbroids of this complex, which host the studied plagiogranites, have $\epsilon_{\text{Nd}}(\text{T}) = -1.8...+0.2$ (Somsikova et al., 2019).

Geological relations of the rocks indicate that the granitoids with adakitic geochemical characteristics were intruded into the dunite–pyroxenite–gabbro series via fracture systems after crystallization and cooling and formation of ophiolite complex. U–Pb zircon dating of tonalite dike from stepped complex of bodies cutting across the dunite–pyroxenite–gabbro banded series of the Sredne-Mamakan ophiolite complex yielded an age of 629 ± 5 Ma (this work), which is

consistent with their geological setting. The values of $\epsilon_{\text{Nd}}(\text{T})$ for two adakitic granitoid samples are +2.5 and +4.0 ($T_{\text{Nd}}(\text{DM})$ account for 0.97 and 0.87 Ga).

A 650–630 Ma stage in the geological history of the Baikal–Muya Belt is reconstructed as subduction setting, which accompanied the formation of the Yakor’ island arc represented by the Yakor’ Sequence, the analogue of the Karalon Sequence (Stanevich and Perelyaev, 1997; Rytsk et al., 2001; Perelyaev, 2003), and subsequent “continental subduction” with formation of eclogite-gneiss complex exposed in the Northern Muya Block (Shatskii et al., 2012, 2014). The Sm–

Nd isochron (garnet, clinopyroxene, and whole-rock) age is 631 ± 17 Ma (Shatsky et al., 2012), while zircon age is 631 ± 9 Ma (Skuzovatov et al., 2019). Eclogites of the Northern Muya block and host gneisses have the following isotope characteristics (Shatsky et al., 2014). The Nd isotope composition of eclogites shows wide variations: $\epsilon_{Nd}(T)$ displays both positive (from +0.3 to +6.9) and negative values (from -0.5 to -16.8). Host gneisses have much narrower variations of Nd ($\epsilon_{Nd}(T)$ from -3.5 to +3.6). Wide variations are also typical of Sr isotope composition of eclogites (0.705043–0.713098). The model age of host gneisses lie within 1.13–1.89 Ma. The isotope data are interpreted by Shatsky et al. as indicating a continental collision in the Baikal–Muya fold belt in the Neoproterozoic, while eclogite gneiss complex of the Northern Muya block marks the paleozone of continental subduction (Shatsky et al., 2014).

Ages of the considered plagiogranites with adakitic affinity (629 ± 5 Ma, this work) and eclogites of the Northern Muya block (631 ± 17 Ma (Shatsky et al., 2012), 631 ± 9 Ma (Skuzovatov et al., 2019) are overlapped within error.

In the Tallain block located in the central part of the Karalon–Mamakan zone, the rocks of the Karalon Sequence are intruded by large 604 ± 17 Ma gabbro–diorite–tonalite intrusive complex (gabbro (Rytsk et al., 2007)), 605 ± 6 Ma granodiorites (Rytsk et al., 2012b)), 612 ± 62 Ma island-arc pyroxenite–gabbro–diorite plutons (Isokh et al., 1998), and 598 ± 4 Ma granites of the Padorin Complex (Rytsk et al., 2007a). Schematic relations between aforementioned magmatic complexes in the eastern Baikal–Muya Belt are shown in Fig. 7a.

The volcanics of the Karalon Group and plagiogranites of the Tallain Complex with erosion are overlain by volcanic rocks of the 590 ± 5 Ma Padrin Complex (Rytsk et al., 2004). The rhyolites and granite porphyry of the Padrin Complex are characterized by $\epsilon_{Nd}(T) = +4.7...+5.4$ ($T_{Nd}(DM)$ accounts for 1.0 Ga). Felsic rocks of the sequence were formed at the beginning of the orogenic stage and are continental volcanic rocks (Rytsk et al., 2004). Granites of the Lesnoy Complex (Fig. 7a) were emplaced at 556 ± 16 Ma. They are characterized by $\epsilon_{Nd}(T) = +3.9$, ($T_{Nd}(DM)$ around 1 Ga) (Rytsk et al., 2001).

The Padrin volcano-plutonic complex is overlain by Late Neoproterozoic volcanoclastic, carbonate–terrigenous molasse sequence of the Mamakan Group (Yakra, Padrokan, Shumninskaya, Delyun–Uran Formation) (Salop, 1964; Stanevich et al., 2007).

Thus, the adakitic plagiogranites emplaced at 629 ± 5 Ma into the rocks of the Sredne-Mamakan ophiolite complex mark the early stage of mafic protolith melting in the Late Neoproterozoic history of the fold belt. Of two generally accepted models of adakite formation (melting of mafic crust in subduction zone or at the base of thick continental crust), the origin of

the considered granitoids is more consistent with the former model, which corresponds to the pre-collisional stage of the evolution of the fold belt.

It was shown for the western Baikal–Muya belt (Fig. 7b) that the plagiogranites of the sheeted and subsheeted bodies with an age of 658–550 Ma (Neimark et al., 1995) were deformed together with amphibolites of the Nyurundukan Sequence. Sm–Nd isochron dating of the amphibolites gave Meso-Neoproterozoic (1035 ± 92 Ma) age, but initial data were not published and were not confirmed later (Rytsk et al., 2007). The granulite metamorphism of mafic rocks ascribed to the Nyurundukan sequence occurred no earlier than 640 ± 5 Ma. The granulites of the Northern Baikal region with an age of 640 ± 5 – 617 ± 5 Ma (Kröner et al., 2015, Amelin et al., 2000) were exhumed into the upper lithosphere horizons by 595 ± 5 Ma. This conclusion was made on the basis of crystallization age of magmatic zircon from vein and dike granitoid bodies of adakitic affinity (Fedotova et al., 2014). Granitoids of this hypabyssal complex have cross-cutting relations with granulites, troctolites, and gabbro of the Tonkiy Cape pyroxenite–troctolite–gabbro complex (Fig. 7b). The Sm–Nd mineral isochron age of the layered complex of this massif is 585 ± 22 Ma (Makrygina et al., 1993). The model age T_{DM} of troctolites of the Tonkiy Cape complex is 0.82–1.29 Ga ($\epsilon_{Nd}(T) = -0.5...+4.9$) (Orlova et al., 2015).

Rytsk et al. (2007) noted that the similar formation age of the eclogites from the eastern branch of the belt and granulites from the western branch indicates a simultaneous occurrence of high-grade metamorphism in the Baikal–Muya Belt.

Based on geochemical characteristics, the tonalite–plagiogranite–granite series ($\epsilon_{Nd}(T) = +3.2...+7.1$) of the hypabyssal complex of the Kichera Zone, eastern Baikal–Muya Belt, occurred, was formed through partial melting of the Neoproterozoic juvenile crust of the island-arc or oceanic type. The Nd isotope composition shows that the crust that experienced partial melting by 595 ± 5 Ma was isotopically and compositionally heterogeneous. The range of $\epsilon_{Nd}(T)$ likely reflects a more heterogeneous composition of crustal protolith compared to that during formation of the adakitic granitoids in the eastern part of the belt.

The accumulation of molasses of the Kholodninskaya Formation and its analogues in the eastern part of the belt in the Late Neoproterozoic (Salop, 1964; Stanevich et al., 2007, and others) marks the cessation of magmatic activity of the Neoproterozoic stage in the evolution of the Baikal–Muya Belt.

CONCLUSIONS

New petrochemical, geochemical, isotope-geochemical and geochronological zircon data were obtained on the postophiolitic granitoid dike system cutting across the dunite–pyroxenite–gabbroic series

of the Sredne-Mamakan ophiolites of the eastern Baikal–Muya Belt. Nd isotope geochemical data were also obtained on the earlier granitoids ascribed to the Sredne-Mamakan ophiolite association of the eastern Baikal–Muya Belt and granitoids of the hypabyssal complex of the Kichera Zone, western Baikal–Muya Belt. Following conclusions were drawn:

(1) The composition and isotope-geochemical characteristics ($\epsilon_{Nd}(T) = -0.9; -1.3$) of plagiogranites from vein bodies no more than 60 cm thick located at the level of leucocratic banded gabbro in the Sredne-Mamakan ophiolite complex are consistent with previously established suprasubduction nature of the ophiolite association.

(2) U–Pb zircon dating of postophiolitic tonalites of the Sredne-Mamakan Complex of the eastern Baikal–Muya folded belt yielded an age of 629 ± 5 Ma.

(3) Sm–Nd isotope-geochemical characteristics of the postophiolitic granitoids from the eastern Baikal–Muya fold belt ($\epsilon_{Nd}(T) = +2.5; +4.0$) in combination with geochemical data confirm the origination of granitoid magmas via partial melting of mafic protolith, which corresponds to the Neoproterozoic oceanic crust.

(4) It was established that the postophiolitic tonalites and plagiogranites of the eastern Baikal–Muya fold belt belong to the adakitic series rocks with high Sr/Y ratios and low Y and HREE contents. Plagiogranite magmas are considered as products of the incipient melting of subducted juvenile Neoproterozoic crust.

(5) In the Kichera zone of the western Baikal–Muya fold belt, adakitic granitoids are ascribed to the differentiated tonalite–leucogranite series of the hypabyssal complex having no direct spatial relation with unambiguous ophiolite associations. The Sm–Nd isotope-geochemical characteristics of these rocks ($\epsilon_{Nd}(T) = +3.2...+7.1$) likely indicate a heterogeneous composition of the Neoproterozoic island-arc or oceanic juvenile crust that experienced partial melting at 595 ± 5 Ma.

ACKNOWLEDGMENTS

We are grateful to S.A. Palandzhyan and G.E. Nekrasov for detailed discussion and important comments that significantly improved the manuscript. We thank V.I. Perelyaev, who provided insight into the geological structure of the Sredne-Mamakan ophiolite association during joint field works, T.I. Kirnozova for help in the optical study of zircon, and M.M. Fuzgan for organization support. E.Yu. Rytsk and its colleagues are grateful for help in the organization of field works in the Northern Baikal region and for unrelenting activity on the geological and geochronological study of the Baikal Mountainous System, which excited us. We are grateful to M.V. Luchitskaya, S.A. Silantsev, and O.M. Turkina for constructive comments that helped in understanding obtained data.

FUNDING

This work was supported by the Russian Foundation for Basic Research (project mol_a 16-35-00600). The studies were carried out in the framework of the government-financed program of the Geological Institute of the Russian Academy of Sciences, theme no. 0135-2019-0051.

REFERENCES

- Yu. V. Amelin, E. Yu. Rytsk, R. Sh. Krymskii, L. A. Neimark, and S. G. Skublov, “Vendian age of enderbite from a granulite complex of the Baikal–Muya ophiolite belt, Northern Baikal Region,” *Dokl. Earth Sci.* **370** (5), 455–457 (2000).
- O. V. Avchenko, N. F. Gabov, and P. V. Kozyreva, et al., “Eclogites of the Northern Muya Block: composition and genesis,” *Izv. Akad. Nauk SSSR. Ser. Geol.*, No. 8, 150–158 (1988).
- P. R. Castillo, “An overview of adakites petrogenesis,” *Chin. Sci. Bull.* **51** (3), 257–268 (2006).
- R. G. Coleman, *Ophiolites* (Springer Verlag, New York, 1977).
- K. C. Condie, “TTG and adakites: are they both slab melts?,” *Lithos* **80**, 33–44 (2005).
- M. J. Defant and M. S. Drummond, “Derivation of some modern arc magmas by melting of young subducted lithosphere,” *Nature* **347**, 662–665 (1990).
- M. J. Defant and P. Kepezhinskas “Evidence suggests slab melting in arc magmas,” *EOS* **82** (6), 65–68 (2001).
- N. L. Dobretsov, “Ophiolites and problems of the Baikal–Muya ophiolite belt,” *Magmatism and Metamorphism of the BAM zone and their Role in the Formation of Mineral Resources* (1983), Vol. 1, pp. 11–19 [in Russian].
- N. L. Dobretsov, E. G. Konnikov, and N. N. Dobretsov, “Precambrian ophiolite belts of southern Siberia, Russia, and their metallogeny,” *Precambrian Res.* **58**, 427–446 (1992).
- M. S. Drummond and M. J. Defant, “A model for trondhjemite–tonalite–dacite genesis and crustal growth via slab melting: Archean to modern comparisons,” *J. Geophys. Res.* **95**, 21503–21521 (1990).
- M. S. Drummond, M. J. Defant, and P. K. Kepezhinskas, “Petrogenesis of slab–derived trondhjemite–tonalite–dacite/adakite magmas,” *Trans. R. Soc. Edinb.: Earth Sci.* **87**, 205–215 (1996).
- S. V. Efremov, “Early Paleozoic adakites in the Eastern Sayan: geochemistry and sources,” *Geochem. Int.* **48** (11), 1112–1127 (2010).
- A. A. Fedotova, A. A. Razumovskiy, E. V. Khain, M. O. Anosova, and A. V. Orlova, “Late Neoproterozoic igneous complexes of the Western Baikal–Muya Belt: formation stages,” *Geotectonics* **48** (4), 292–312 (2014).
- H. Furnes and Y. Dilek, “Geochemical characterization and petrogenesis of intermediate to silicic rocks in ophiolites: a global synthesis,” *Earth–Sci. Rev.* **166**, 1–37 (2017).
- N. F. Gabov, N. L. Dobretsov, and V. G. Kushev, “Eclogites and eclogite–like rocks in the Northern Baikal region,” *Petrology and Mineralogy of the Mafic Rocks of*

- Siberia* (Nauka, Moscow, 1984), pp. 36–50 [in Russian].
- A. E. Izokh, A. S. Gibsher, D. Z. Zhuravlev, and P. A. Balykin, “Sm–Nd dating of the ultramafic–mafic massifs of the eastern branch of the Baikal–Muya ophiolite belt,” *Dokl. Earth Sci.* **360** (1), 525–529 (1998).
- S. E. Jackson, N. J. Pearson, W. L. Griffin, and E. A. Belousova, “The application of laser ablation–inductively coupled plasma–mass spectrometry to in situ U–Pb zircon geochronology,” *Chem. Geol.* **211**, 47–69 (2004).
- E. V. Khain, E. B. Sal’nikova, A. B. Kotov, K.–P. Burgath, A. A. Fedotova, V. P. Kovach, S. Z. Yakovleva, D. N. Remizov, and F. Schaefer, “U–Pb age of plagiogranites from the ophiolite association in the Voykar–Synya massif, Polar Urals,” *Dokl. Earth Sci.* **419** (3), 392–396 (2008).
- K. A. Klitin, E. A. Domina, and G. V. Rile, “Structure and age of the ophiolite complex of the Baikal–Vitim Rise,” *Byul. Mosk. O-va Ispyt. Prir., Nov. Ser., Otd. Geol.* **80** (1), 82–94 (1975).
- E. G. Konnikov and A. A. Tsygankov, “Heterogeneity of the Baikal–Muya ophiolite belt,” *Dokl. Akad. Nauk* **327** (1), 115–120 (1992).
- E. G. Konnikov, V. F. Posokhov, and T. T. Vrublevskaya, “Genesis of plagiomigmatites in the Precambrian ophiolites of Northern Baikal region,” *Geol. Geofiz.*, No. 1, 82–88 (1994).
- E. G. Konnikov, A. A. Tsygankov, and T. T. Vrublevskaya, “Baikal–Muya Volcanoplutonic Belt: Lithotectonic Complexes and Geodynamics (GEOS, Moscow, 1999) [in Russian].
- Yu. A. Kostitsyn and A. Z. Zhuravlev, “Error analysis and optimization of isotope dilution method,” *Geokhimiya*, No. 7, 1024–1036 (1987).
- Yu. A. Kostitsyn and M. O. Anosova, “U–Pb age of extrusive rocks in the Uxichan Caldera, Sredinnyi Range, Kamchatka: application of laser ablation in dating young zircons,” *Geochem. Int.* **51**(2), 155–163 (2013).
- A. Kröner, A. A. Fedotova, E. V. Khain, et al., “Neoproterozoic ophiolite and related high–grade rocks of the Baikal–Muya belt, Siberia: geochronology and geodynamic implications,” *J Asian Earth Sci.* **111**, 138–160 (2015).
- M. V. Luchitskaya, “Interrelation between granitoid accretionary and adakite magmatism at the Pacific active margin,” *Dokl. Earth Sci.* **385** (2), 525–529 (2002).
- K. R. Ludwig, “Isoplot 3.75: A geochronological toolkit for Microsoft Excel,” *Spec. Publ. Berkeley Geochronol. Center*, no. 5 (2012). V. A. Makrygina, A. A. Koneva, and L. F. Piskunova, “Granulites in the Nyurundukan Series of the Northern Baikal region,” *Dokl. Akad. Nauk SSSR* **307** (1), 195–201 (1989).
- V. A. Makrygina, E. G. Konnikov, L. A. Neimark, et al., “On the age of the granulite–charnockite complex in the Nyurundukan Group of the Northern Baikal region: a paradox of radiochronology,” *Dokl. Akad. Nauk* **332** (4), 486–489 (1993).
- H. Martin, R. H. Smithies, R. Rapp, J. F. Moyen, and D. Champion, “An overview of adakite, tonalite–trondhjemite–granodiorite (TTG), and sanukitoid: relationships and some implication for crustal evolution,” *Lithos* **79**, 1–24 (2005).
- L. A. Neimark, E. Yu. Rytsk, B. M. Gorokhovskii, et al., “On the age of the “Muya” granites of the Baikal–Vitim ophiolite belt: U–Pb– and Sm–Nd–isotope data,” *Dokl. Akad. Nauk* **343** (5), 673–676 (1995).
- A. V. Orlova, A. A. Razumovskii, N. M. Revyako, et al., “Affiliation of the Tonky Cape massif to the Chaya–Nyurundukan ultramafic–mafic complex, Northern Baikal region: Sm–Nd data,” *Isotope Dating of Geological Processes: New Results, Approaches, and Prospects. 6th All-Russian Conference on Isotope Geochronology* (IGGD RAS, St. Petersburg, 2015), pp. 204–206 [in Russian].
- L. M. Parfenov, A. I. Khanchuk, et al., “Model of formation of orogenic belts of Central and Northeastern Asia,” *Tikhookean. Geol.* **22** (6), 7–41 (2003).
- L. M. Parfenov, G. Badarch, N. A. Berzin, et al., “Tectonic and metallogenic model for Northeast Asia,” *Metallogenesis and Tectonics of Northeast Asia*, Ed. by W. J. Nokleberg, U.S. Geol. Surv. Prof. Pap. **1765**, 9–1–9–55 (2010).
- V. I. Perelyaev, Extended Abstract of Candidate’s Dissertation in Geology and Mineralogy (IZK SO RAS, Irkutsk, 2003) [in Russian].
- N. Petford and M. Atherton, “Na–rich partial melts from newly underplated basaltic crust: the Cordillera Blanca Batholith, Peru,” *J. Petrol.* **37** (6), 1491–1521 (1996).
- J. A. Pfänder, K. P. Jochum, I. Kozakov, et al., “Coupled evolution of back–arc and island arc–like mafic crust in the late–Neoproterozoic Agardagh Tes–Chem ophiolite, Central Asia; evidence from trace element and Sr–Nd–Pb isotope data,” *Contrib. Mineral. Petrol.* **143**, 154–174 (2002).
- N. M. Revyako, Yu. A. Kostitsyn, and Ya. V. Bychkova, “Interaction between a mafic melt and host rocks during formation of the Kivakka layered intrusion, North Karelia,” *Petrology* **20** (2), 101–119 (2012).
- A. V. Ryazantsev, G. N. Savelieva, and A. A. Razumovsky, “Dike complexes in ophiolites of the Urals,” *Geotectonics* **49** (3), 36–55 (2015).
- E. Yu. Rytsk, Yu. V. Amelin, N. G. Rizvanova, R. Sh. Krimsky, G. L. Mitrofanov, N. N. Mitrofanova, V. I. Perelyaev, and V. S. Shalae, “Age of rocks in the Baikal–Muya Foldbelt,” *Stratigraphy. Geol. Correlation* **9** (4), 315–326 (2001).
- E. Yu. Rytsk, A. F. Makeev, V. A. Glebovitsky, and A. M. Fedoseenko, “A Vendian (590 ± 5 Ma) age for the Padora Group in the Baikal–Muya Foldbelt: evidence from U–Pb Zircon data,” *Dokl. Earth Sci.* **397** (6), 765–767 (2004).
- E. Yu. Rytsk, A. F. Makeev, V. A. Glebovitsky, and A. M. Fedoseenko, “Early Vendian Age of multiple gabbro–granite complexes of the Karalon–Mamakan Zone, Baikal–Muya Belt: new U–Pb zircon data,” *Dokl. Earth Sci.* **415A** (6), 911–914 (2007a).
- Rytsk E. Yu., V. P. Kovach, V. I. Kovalenko, and V. V. Yarmolyuk, “Structure and evolution of the continental crust in the Baikal Fold Region,” *Geotectonics* **41** (6), 440–464 (2007b).
- E. Yu. Rytsk, A. B. Kotov, E. B. Salnikova, et al., “U–Pb geochronology of the gabbro–diorite–tonalite–granodiorite intrusions of the Baikal–Muya belt,” *Geody-*

- namic Evolution of Lithosphere of the Central Asian Orogenic Belt: from Ocean to Continent* (IZK SO RAN, Irkutsk, 2012), vol. 2, p. 57 [in Russian].
- L. I. Salop, *Geology of the Baikal Mountainous Region* (Nedra, Moscow, 1964) [in Russian].
- G. N. Savelieva, N. S. Bortnikov, T. B. Bayanova, et al., “Sm–Nd and Rb–Sr isotopic systems and captured He and hydrocarbon gases as markers of melt sources and fluid regime under which the oceanic crust of the Mid–Atlantic Ridge was formed at 5°–6° N,” *Geochem. Int.* **46** (8), 745–758 (2008).
- V. S. Shatsky, E. S. Sitnikova, A. A. Tomilenko, A. L. Ragozin, O. A. Koz'menko, and E. Jagoutz, “Eclogite–gneiss complex of the Muya block (East Siberia): age, mineralogy, geochemistry, and petrology,” *Russ. Geol. Geophys.* **53** (6), 501–521 (2012).
- V. S. Shatsky, S. Yu. Skuzovatov, A. L. Ragozin, and S. I. Dril, “Evidence of Neoproterozoic continental subduction in the Baikal–Muya Fold Belt,” *Dokl. Earth Sci.* **459** (2), 1442–1445 (2014).
- S. A. Silantyev, J. Koepke, A. A. Ariskin, M. O. Anosova, E. A. Krasnova, E. O. Dubinina, and G. Suhr, “Geochemical nature and age of the plagiogranite–gabbro–norite association of the oceanic core complex of the Mid–Atlantic Ridge at 5°10'S,” *Petrology* **22** (2), 109–127 (2014).
- E. V. Sklyarov, V. P. Kovach, A. B. Kotov, et al., “Boninites and ophiolites: problems of their relations and petrogenesis of boninites,” *Russ. Geol. Geophys.* **57** (1), 127–140 (2016).
- S. Skuzovatov, V. Shatsky, and K. L. Wang, “Continental subduction during arc–microcontinent collision in the southern Siberian craton: Constraints on protoliths and metamorphic evolution of the North Muya complex eclogites (Eastern Siberia),” *Lithos* **342–343**, 76–96 (2019).
- A. V. Somsikova, A. A. Fedotova, V. I. Perelyaev, et al., “New Rb–Sr and Sm–Nd isotope–geochemical data on the rocks of the Srednemamakan ophiolite complex of the eastern Baikal–Muya fold belt,” *Proc. 22th Vinogradov Symposium on Isotope Geochemistry* (GEOKHI RAS, Moscow, 2019), p. 84 [in Russian].
- N. A. Srytsev, V. A. Khalilov, V. V. Buldygerov, and V. I. Perelyaev, “Geochronology of granitoids of the Baikal–Muya belt,” *Geol. Geofiz.*, No. 9, 72–78 (1992).
- A. M. Stanevich and V. I. Perelyaev, “On Late Precambrian stratigraphy of the Sredne Vitim mountainous country,” *Geol. Geofiz.* **38** (10), 1642–1652 (1997).
- A. M. Stanevich, A. M. Mazukabzov, A. A. Postnikov, V. K. Nemerov, S. A. Pisarevsky, D. P. Gladkochub, T. V. Donskaya, and T. A. Kornilova, “Northern segment of the Paleasian ocean: Neoproterozoic deposition history and geodynamics,” *Russ. Geol. Geophys.* **48** (1), 46–60 (2007).
- S. S. Sun and W. F. McDonough, “Chemical and isotopic systematics of oceanic basalts: implications for mantle composition and processes,” *Magmatism in Ocean Basins*, Ed. by A. D. Saunders and M. J. Norry, *Geol. Soc. Spec. Publ.* **42**, 313–345 (1989).
- T. Tanaka, S. Togashi, H. Kamioka, et al., “JNdi–1: a neodymium isotopic reference in consistency with LaJolla neodymium,” *Chem. Geol.* **168** (3–4), 279–281 (2000).
- B. Taylor and E. Martinez, “Back–arc basin basalt systematics,” *Earth Planet. Sci. Lett.* **210** (3–4), 481–497 (2003).
- S. R. Taylor and S. M. McLennan, *The Continental Crust: Its Composition and Evolution* (Blackwell Scientific, Oxford, 1985).
- A. A. Tsygankov, “Metavolcanic rocks of the Baikal–Muya Ophiolite belt: geochemistry and correlation,” *Geol. Geofiz.* **39** (9), 1133–1147 (1998).
- A. A. Tsygankov, *Magmatic Evolution of the Baikal–Muya Volcanoplutonic Belt in the Late Precambrian* (SO RAS, Novosibirsk, 2005) [in Russian].
- O. M. Turkina, “Tonalite–trondhjemite complexes of the suprasubduction settings: evidence from the Late Rhiphean plagiogranitoids of the SW margin of the Siberian Platform,” *Geol. Geofiz.* **43** (5), 418–431 (2002).
- E. van Achterbergh, C. G. Ryan, and W. L. Griffin, “GLITTER: On–line interactive data reduction for the Laser Ablation ICP–MS microprobe,” *Proceedings of the 9th V.M. Goldschmidt Conference* (Cambridge, 1999), p. 305.
- A. E. Vladimirov, N. K. Korobeinikov, and I. V. Chetverikov, *State Geological Map of the Russian Federation on a Scale 1 : 200000, 2nd Ed., Muya Series, Sheet O–50–XXV and Explanatory Note* (VSEGEI, St. Petersburg, 2004) [in Russian].
- M. Wiedenbeck, P. Allé, F. Corfu, et al., “Three natural zircon standards for U–Th–Pb, Lu–Hf, trace element and REE analyses,” *Geostand. Newslett.* **19** (1), 1–23 (1995).
- J. F. Xu, R. Shinjo, M. J. Defant, et al., “Origin of Mesozoic adakitic intrusive rocks in the Ningzhen area of east China: Partial melting of delaminated lower continental crust?,” *Geology* **30** (12), 1111–1114 (2002).

Translated by M. Bogina